Univerzita Tomáše Bati ve Zlíně
Fakulta technologická
Ústav inženýrství polymerů
akademický rok: 2006/2007

ZADÁNÍ DIPLOMOVÉ PRÁCE

(PROJEKTU, UMĚLECKÉHO DÍLA, UMĚLECKÉHO VÝKONU)

Jméno a příjmení:	**Bc. Marta HRABALOVÁ**
Studijní program:	**N 2808 Chemie a technologie materiálů**
Studijní obor:	**Inženýrství polymerů**
Téma práce:	**Photodegradation of beta-nucleated polypropylene: the effect of structure parameters**

Zásady pro vypracování:

The aim of this Master thesis is to verify the effect of molecular structure on photodegradation of neat and beta-nucleated polypropylene. Polypropylenes with different melt flow index will be UV-irradiated and then examined by several methods. Infrared spectroscopy, X-ray scattering and differential scanning calorimetry will be employed.

Rozsah práce:

Rozsah příloh:

Forma zpracování diplomové práce: **tištěná/elektronická**

Seznam odborné literatury:

Wypych, G.: Handbook of Material Weathering (2nd Edition), ChemTec Publishing, 1995, ISBN: 1-895198-12-7

Wypych, G.: Weathering of Plastics – Testing to Mirror Real Life Performance, William Andrew Publishing/Plastics Design Library, 1999, ISBN: 1-884207-75-8

Karger-Kocsis, J.: Polypropylene – An A-Z Reference, Springer -- Verlag, 1999, ISBN: 0-412-80200-7

Maier, C.; Calafut, T.: Polypropylene – The Definitive User's Guide and Databook, William Andrew Publishing/Plastics Design Library, 1998, ISBN: 1-884207-58-8

and scientific articles

Vedoucí diplomové práce: **Ing. Jana Výchopňová**
Ústav inženýrství polymerů

Datum zadání diplomové práce: **11. listopadu 2006**

Termín odevzdání diplomové práce: **10. května 2007**

Ve Zlíně dne 5. února 2007

prof. Ing. Ignác Hoza, CSc.
děkan

UNIVERZITA TOMÁŠE BATI VE ZLÍNĚ
Fakulta technologická
L.S.

prof. Ing. Milan Mládek, CSc.
ředitel ústavu

ACKNOWLEDGEMENT

I would like to thank my supervisor Jana Výchopňová for her professional, reliable, rigorous and promt help in the course of full time of my work. In the same way the expression of thanks goes to the Sophie Commereuc for her care and advices.

I declare I worked on this Master thesis by myself and I have mentioned all the used literature.

Zlín, 21. května 2007

_____

jméno

ABSTRACT

This master thesis probes the possible options of influence of melt flow rate on photooxidative degradability of neat polypropylene and polypropylene containing β-nucleating agent based on N,N'-dicyclohexyl-2,6-naphtalenedicarboxamide in the amount of 0.03 wt.%. Five commercial grades of polypropylene differing in melt flow index were exposed to the UV-radiation for several exposition durations and consequently the changes accrued in these samples were progressively monitored by infrared spectroscopy, differential scanning calorimetry, X-ray diffraction and optical microscopy. The results showed that the β-nucleation significantly enhanced the stability of polypropylene against UV-light. However, the melt flow rate was not found to play an important role it the process of photooxidation.

Keywords: isotactic polypropylene, polymorphism, β-form, α-form, photooxidation, melt flow index

ANOTACE

Tato diplomová práce zkoumá možnosti vlivu velikosti indexu toku taveniny polypropylenu bez obsahu nuklečního činidla a polypropylenu obsahujícího β-nukleační činidlo (na bázi N,N'-dicyklohexyl-2,6-naftalendikarboxamidu v množství 0,03 hm.%) na fotooxidační degradabilitu. Pět komerčně využívaných druhů polypropylenu lišících se v hodnotě indexu toku taveniny byly vystaveny UV-záření v různě dlouhých časových intervalech. Změny, které se vyskytly ve vzorcích byly postupně sledovány s použitím infračervené spektroskopie, diferenciální snímací kalorimetrie, rentgenografie a optickou mikroskopií. Výsledky ukázaly, že β-nukleace výrazně zlepšuje stabilitu polypropylenu vůči UV-záření. Vyšlo na jevo, že velikost indexu toku taveniny nemá jednoznačný vliv na fotodegradaci tohoto materiálu.

Klíčová slova: izotaktický polypropylen, polymorfismus, β-fáze, α-fáze, fotooxidace, index toku taveniny

TABLE OF CONTENT

INTRODUCTION

Polymers enclose us as a relatively new class of materials when supply the natural materials by applying their advantageous properties. In recent years a lot of effort has been invested to improve these qualities, reduce the cost, enlarge the application regarding the influence of these materials on the environment and other way round. Presently there is a huge amount of the variants of polymers differing in the composition and the structure and these materials are furthermore mixed or filled by the distinct admixtures. When studying the utilization of polymers adherent to the persistence all these aspects has to be taken into the consideration.

The polyolefins are the sort of the largest sales volume polymers. Polypropylene is the one of the polyolefin category and it is widely used in many industrial branches. This material appears in several modifications and adjustments. The most common build of polypropylene is the isotactic. Some polymers are rich in the structure possibilities and polypropylene is not excepted. By using varied preparation procedures isotactic polypropylene exhibits four morphological forms on the crystal lattice: α (monoclinic), β (trigonal), γ (orthorombic) and smectic. Similar variations are acceptable also for other crystalline polymers, hence, they are called polymorphic.[1, 2, 3] In sequence of the structure divergence of isotactic polypropylene the feature differences of this material appears as well as the difference in response on the external agencies, primarily the UV radiation.

The influence of the UV light upon the isotactic polypropylene causes the most significant changes, when compared to the other possible environmental actions such as the temperature, chemicals and the microorganisms, that have ultimately negative fallout on the mechanical endurance and the appearance of the polypropylene.

The effect of structure parameters on UV-degradation of the β-nucleated polypropylene has to be taken into consideration. As mentioned α- and β-forms of isotactic polypropylene differ in many ways. The basic and the most common form of polypropylene is α-form, appeared to be less profitable than the β-form in some applications. These forms also behave unlikely upon UV–exposition. β-form degrades slower than α-form.[4] Nevertheless, the influence of the molecular structure of isotactic polypropylene on its photodegradation, regardles of the presence of β-nucleating agent in the material, could be also expected.

Considering these facts this work is to compare and describe the process of photooxidation of neat and β–nucleated polypropylenes with different molecular weights (different melt flow index) by common examining methodes such as infrared spectroscopy, X-ray diffraction, differential scanning calorimetry and light microscopy.

I. THEORETICAL PART

1 POLYPROPYLENE

Polypropylene (PP) is one of the major polymers. It is a linear hydrocarbon polyolefin or saturated polymer. This material was introduced to the large scale production in 1957 as a plastic and fibre forming material.[5]

1.1 PRODUCTION

Polypropylene is produced by propylene monomer (CH_2=CH–CH_3). Propylene is colorless gas, practically odorless (boiling point -47.6 °C, melting point –185.2 °C). It is produced primarily as a by product of petroleum refining and of ethylene production by steam cracking of hydrocarbon feedstocks. Propylene is major chemical intermediate. In the environment, propylene occurs as a natural product of vegetation.[6]

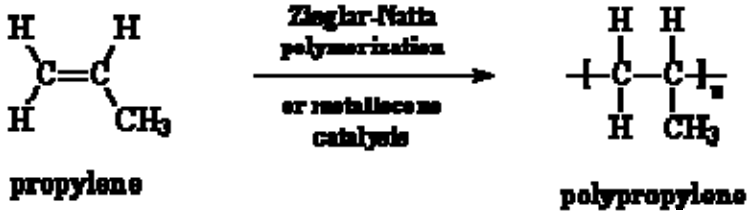

Fig. 1: Ziegler-Natta polymerization[7]

The polypropylene was first synthetized in 1869 by Barthelot. It was sticky sediment and had no possible application for industry. The possibility of the production of the highly stereoregular polymer (isotactic or syndiotactic) appeared at the beginning of the 1950s. Karl Ziegler discovered compounds which lead monomer to the fast polymerization at the low pressure. The original Ziegler-Natta catalysts were a complex of transition metal halides, with an organometallic compound, as cocatalyst to initiate the polymerization. These catalysts provide active sites or polymerization sites where the polymerization reaction occurs, by holding the growing polymer chain and the propylene monomer in close proximity to each other so that they can react (Fig.1).

Because of the low yield, supported heterogeneous Ziegler-Natta catalysts were developed in the 1960s, with magnesium dichloride ($MgCl_2$) used as the inert support material. These were added to control the polymer growth. The addition of Lewis base supported catalyst activity and stereospecificity and eliminated the necessity of post reactor removal of catalyst residues. Catalyst systems using newer Lewis bases further increased isotacticity and activity and are currently used in the industrial production of polypropylene.

In the search for a deeper understanding and control of Ziegler-Natta polymerization at the molecular level, a number of metallocene catalysts have been developed. Current metallocene catalyst systems commonly use zirconium chloride ($ZrCl_2$) as the transition metal complex, with a cyclopentadiene as the organic compound and an aluminoxane such as cocatalyst. These catalysts are even more effective to produce highly stereoregular polypropylene and polyolefins in general.

By using metallocene cytalysts, the homogeneous stereo-regular polypropylene is produced, thus the property profile of the material is easier to control.[8] Moreover, these catalysts made commercial production of sydndiotactic polypropylene possible.[9]

1.2 CHEMICAL STRUCTURE

The basic building unit is a repeating unit of propylene. The main chain is composed of the carbon atoms. Every other of them carries a methyl group. There are three types of PP according to the position of the methyl group: isotactic, syndiotactic and atactic.

The stereochemical structure of PP is demonstrated with the planar form trans. The atoms of the chain are stowed in a basic chain plain sandwiching.

1.2.1 Atactic polypropylene

In atactic polypropylene (aPP) pendant methyl groups are oriented randomly with respect to the polymer backbone (Fig.2).[9]

Generally atactic polymers are characterized by their tacky, amorphous behaviour (they are unable to crystallize) and low molecular weights. Atactic portion provide the same effect as a plasticizer, by reducing the crystallinity of the polypropylene. A small amount of atactic polymers in the final polymer can be used to improve certain mechanical properties. This provides properties to the

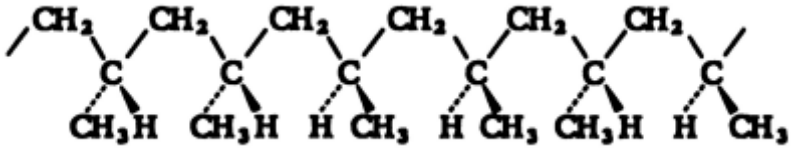

Fig. 2: Atactic polypropylene[10]

final polymer, such as improved low temperature performance, elongation, processability and optical properties (transparency), but sacrifices flexural modulus or stiffness, and long-term heat ageing properties. Configuration of atactic polypropylene is randomly distributed in the repeat units. The structure is irregular, the polymer is weak rubber compared with the isotactic polypropylene, which is hard and stiff. It is utilizated as a carpet backing, adhesives, roofing tars[9] and road surfacing material.[5]

1.2.2 Syndiotactic polypropylene

In syndiotactic polypropylene (sPP), middle, consecutive pendant methyl groups are on opposite sides of the polymer backbone chain (Fig.3).[9]

Sequence for each syndiotactic unit sets up a helix with two syndiotactic units per turn with a period of 0.74 nm. The stable structure of sPP has a unit cell which includes 2 left– and 2 right–handed helices in a regular alternation along both the *a* and the *b* axis. In real crystals the regular left-right packing is often dislocated, leading to lattice disorder. This disorder is known to increase with decreasing crystallization temperature (T_c).[11] Syndiotactic polypropylene forms both hedrites and spherulites, depending on the T_c. Going to lower T_c, an increasing tendency of branching and splaying of growing lamellae continuously changes the hedrites into spherulites.[11] Compared to isotactic polypropylene the

crystallinity of sPP is very low. The development of spherulites occurs at lower temperature then that in isotactic polypropylene, their size is much lower.[12]

The ability to synthetize highly stereoregular sPP was realized around 1990 by the use of metallocene catalysts. Metallocene-catalyzed synthesis of PP lead to the well controlled tacticity and molecular weight distribution.[13]

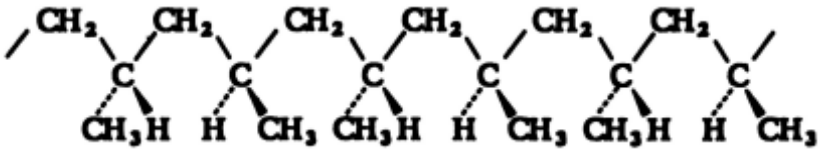

Fig. 3: Syndiotactic polypropylene[10]

The syndiotactic polypropylene crystallizes with a melting temperature value 134 °C, the equilibrium melting temperature (T_m°) is 183 °C and has a glass transition temperature (T_g) value of about 0 °C.

Syndiotactic polypropylene is less stiff than isotactic polypropylene but has better impact strength and clarity. Syndiotactic polypropylene finally found the application in adhesives, caulks, and cable-filling compounds.[5]

1.2.3 Isotactic polypropylene

In isotactic polypropylene (iPP) the pendant methyl groups branching off from the polymer backbone are all on the same side of the polymer backbone, with identical configurations relative to the main chain (Fig. 4).[9]

In iPP, the chain adopts a 3_1-helix, a three-fold helix which indicates that it takes three monomer units to make one helical turn. The helix can be either right (R)- or left (L)-handed, with a period of 0.65 nm as shown in Fig 5. The right- and left-handedness are related by a mirror symmetry parallel to the helix.

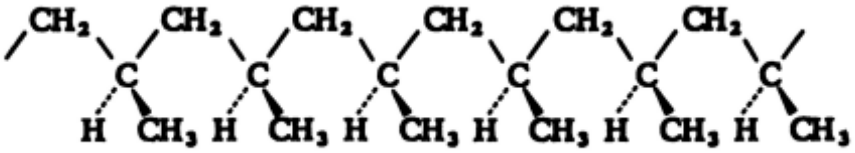

Fig. 4: Isotactic polypropylene[10]

Furthermore the orientation of the CH_3 group with respect to the chain axis can be either up or down. The up and down conformations overlap each other if rotated by 180° around the normal of the chain axis. As a consequence four possible configurations can be distinguished relative to their reference axis as shown in Fig. 5.[10]

Due to its tacticity, iPP is the most stereo-regular structured polypropylene when compared to aPP and sPP and thus higher degree of crystallinity (60–70 %) is involved. Increased crystallinity of PP results in good mechanical properties such as stiffness and tensile strength. This allows polypropylene to be used as a replacement for engineered thermoplastics, such as ABS.[14]

Molecular weight of iPP is from 100 000 to 600 000 g/mol, melting temperature (T_m) is 170 °C and the density is ρ=0.905–0.912 g/cm^3.[1, 2, 3]

1.3 MORPHOLOGY OF ISOTACTIC POLYPROPYLENE

By using varied preparation procedures, iPP exhibits three different morphological forms on the crystal lattice: α (monoclinic), β (trigonal), and γ (orthorhombic), distinguished by the arrangement of the chains.[15-20] Another form of iPP with degree of order between crystalline and amorphous phases is called „smectic“ and was first reported by Natta. This variety in morphology is called polymorphism which is a common phenomenon in crystalline polymers.[1, 2, 3]

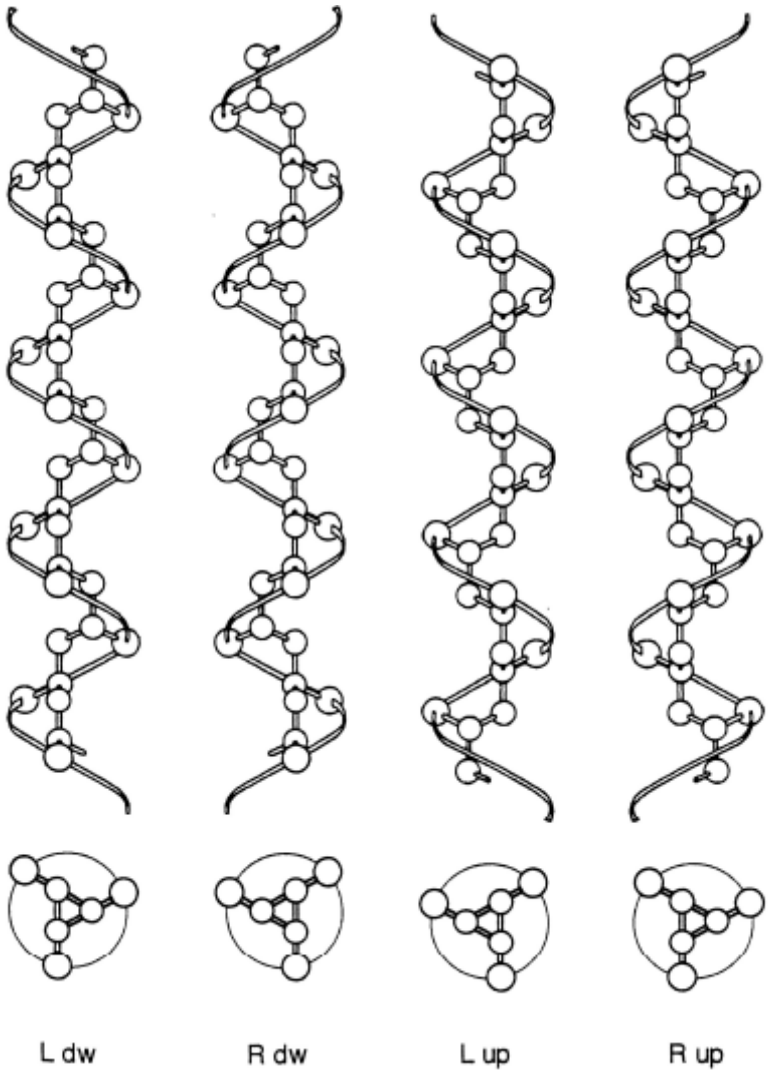

Fig. 5: Chain conformations of isotactic polypropylene. Right (R)- and Left (L)- handed 3_1 helices in their up (up) and down (dw) configurations[21]

1.3.1 α-form

The predominant and most thermodynamically stable crystalline structure of pure isotactic polypropylene at atmospheric pressure is monoclinic α structure (α-iPP). Unit cell parameters are: *a*=0.665 nm, *b*=2.096 nm, *c*=0.650 nm with α=β=90°, and γ=99.3°. The density of this polypropylene form is 0.94

g/cm^3.[22, 23] A model of α-form crystal structure is schemed in Fig. 6. The boundary between α-spherulites is shown in Fig. 7.

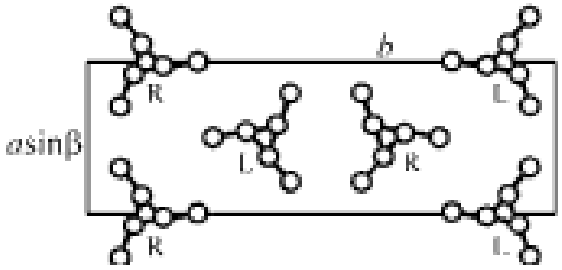

Fig. 6: α-form of iPP[21]

The α-form of iPP exhibits three types of spherulites:

- α_I-positive birefringence spherulites; developed at an isothermal crystallization temperature below 132 °C
- α_{II}-negative birefringence spherulites; exist at a temperature greater than 138 °C
- α_{III} or α_m-mixed birefringence spherulites; no distinct Maltese cross; revealed as radiating arrays of intermingled areas of positive and negative birefringence; observed at any temperature up to 152 °C.

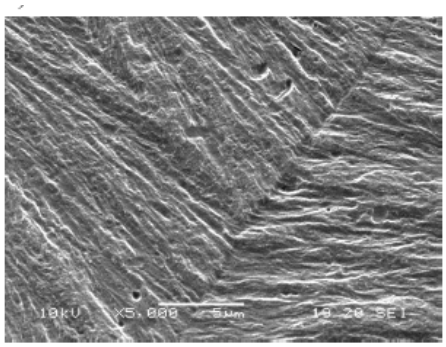

Fig. 7: Scanning electron microscopy micrograph of α-spherulites[24]

The presence of one type depends not only on the crystallization temperature, but also on the film thickness. The birefringence change of α-form spherulites has been directly related to the relative amounts of tangential lamellae branching, inside the spherulites. An amount of branching lamellae is relatively higher in positively birefringent α_I than that in the negatively birefringent α_{II}. The angle between branched lamellae for twin crystals grown by crystallization in solution is about 80 °.[3]

The presence of mentioned thin lamellar branches inclined at 80 ° to the dominant radial lamellae complicates the melting behaviour of α-spherulites of iPP. During a heating cycle the branches melt at lower temperature than dominant lamellae, causing an increase in the birefringence of the spherulites and, hence, of the specimen. Values of the equilibrium melting temperature reported in the literature fall into two groups, one around 186 °C and the other around 210 °C.[25]

1.3.2 β-form

The β-form of iPP was first identified in 1959 by Keith et al.[26] It is often referred in literature as a „hexagonal iPP" as it was first described but in fact crystal structure of β-modification was latterly estabilished as a trigonal unit cell with parameters $a=b$=1.01 nm, c=6.5 nm, $\alpha=\beta$=90° and γ=60° (Fig.8).[27] The density of β-form is 0.92 g/cm^3.[28]

In conventional iPP grades a small amount of β-form occurs sporadically at high supercoolings (T_c<130 °C) or in quenched samples. It is possible to produce a high amount of β-form using special crystallization conditions such as crystallization in temperature gradient or shear stress.[10] However, the most reliable way to prepare the β-form is by using special β-nucleating agents. The first of them was identified in 1967 (Permanent Red E3B-quanacridone) and later the other, more efficient, types of β-nucleators were identified such as alkali metal and di-acid compound.[29] Recently, the commercial β-nucleating agent NJ Star NU 100 based on N,N'-dicyclohexylnaphthalene-2,6-dicarboxamide (NU 100) has attracted the attention of many papers.[30-34]

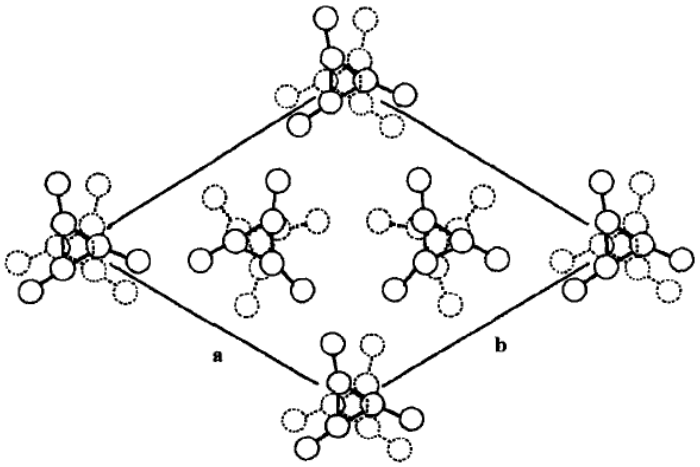

Fig. 8: The unit cell and structure of β-iPP[28]

An interesting feature of the growth of the β-form is the β to α modification transition. It can be generally stated that this transition always takes place if the growth rate of the α-form (G_α) is higher than that of the β-form (G_β). It was found, that the temperature interval where the G_β exceeds G_α is limited by higher limit temperature $T(\beta\alpha)$ and lower limit temperature $T(\alpha\beta)$.[35-37] The phenomenon of β to α growth transition above $T(\beta\alpha)$ and below $T(\alpha\beta)$ which takes place on the growing β-crystal front evidences that the formation of pure β-form has a theoretical upper ($T(\beta\alpha)$=140−141 °C) and a lower limit temperature ($T(\alpha\beta)$~105 °C). Within this temperature interval different types of supermolecular structures (SMS) of β-nucleated polypropylene (β-iPP) can be formed. The types and structural features of SMS formed are markedly influenced by the thermal conditions of crystallization, by the melt history,[39] by mechanical stresses to the crystallizing system and by the presence of extraneous materials. In a quiescent melt, β-spherulites can be formed. Depending of the crystallization temperature, negative radial (grow below 128 °C) or negative banded (grow between 128 and 135 °C) β-spherulites of iPP might form during the melt crystallization. The β-spherulites have strong negative birefringence in comparison with the α-spherulites.[39, 40] The texture of β-spherulites is shown in the Fig. 9.

Similar to the α-form, many values of the equilibrium melting point have been reported; [25] it varies from 170 to 200°C. The value of 174.4 °C for T_m° was reported using the same procedure for determining the most accurate value T_m° of the α-form.[25]

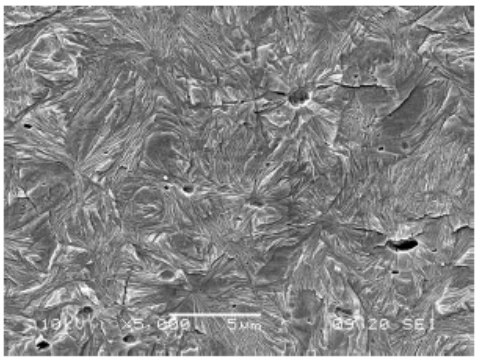

Fig. 9: Scanning electron microscopy micrograph of β-spherulites[37]

Overall the studies shows that β-form is less stable and tends to turn into the α-form when subjected to external parameters such as heat (as written above) or even force.[29] Padden and Keith[39] demonstrated that β-spherulites recrystallize into α-form (βα-recrystallization) when heated and, finally, they melt from this form. Hence, due to this recrystallization phenomenon and melting of the α- and β-forms of iPP with mixed polymorphic content, the melting curves have a complicated melting profile.[41-43] According to Varga,[30, 40, 44] the melting characteristics of β-iPP are highly sensitive to the post-crystallization thermal history (melting memory effect). It can be stated that β-iPP samples are susceptible to βα-recrystallization only if they were cooled below a critical temperature before melting. This critical recooling temperature is T_R^*~100−105 °C. It should be suggested, that the critical recooling temperature corresponds to the lower limit temperature, $T(\alpha\beta)$, of the formation of pure β-iPP.

It was found, that iPP rich in β-form embodies improvement of some mechanical properties. In particular the impact strength, toughness and whitening under tensile deformation of β-iPP markedly exceed those of polypropylene with predominant α-form.[24] However, the presence of β-form in the material decreases stiffness and E-modulus.

1.3.3 γ-form

This form was discovered in 1961 by Addink & Beintema.[24] It was produced by crystallization at elevated pressures from high molecular weight homopolymer.[25] The γ-form predominates when the pressure during the crystallization is higher than 200 MPa. Other procedure which leads to the growth of this form is crystallization from the melt of high molecular weight stereoblock copolymer with small amounts of ethylene or but-1-ene.

The orthorhombic structure of γ-form was proposed by Brückner and Meille and is schematically shown in Fig. 10. The lattice parameters of the cell are *a*=0.854 nm, *b*=0.993 nm and *c*=4.241 nm.[25] The density of γ-form is the same as the density of α-form.[28]

The overall architeture of γ-form is very unusual. The chain axes in the crystal are not aligned in one direction as in other polymer crystals. Instead, the

chain form alternating layers of parallel chain ordering. The angle between the chain directions in two consecutive layers is approximately 80 °, the branching is

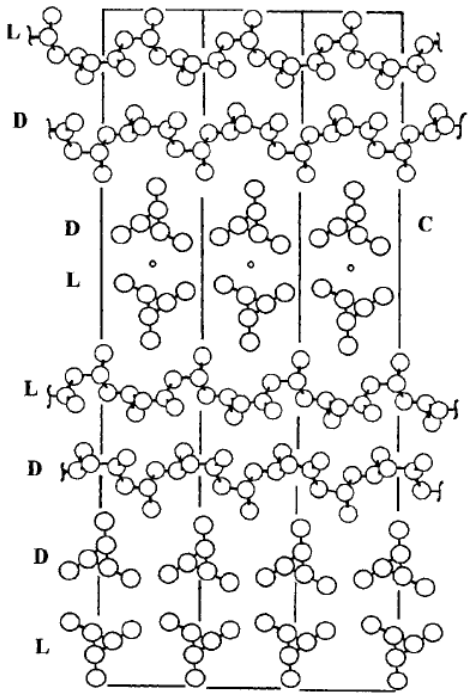

Fig. 10: The structure of γ-iPP viewed along the chain axis of macromolecules belonging to one bilayer[45]

similar to that in the α-form.[24] There is an relation between α-form and γ-form. It was found that α-form lamellae, which crystallize at higher temperatures than that of γ-form, can act as a nucleus for the γ-form. This is called epitaxial crystallization of the γ-form on α-lamellae.[10] Packing energy calculations showed that γ-form is at least as stable as α-form. The spherulite structure of γ-form is viewed in Fig. 11.

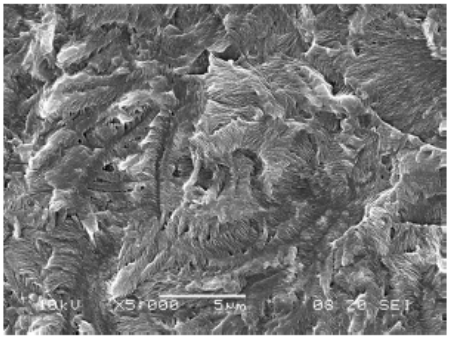

Fig. 11: SEM micrograph feather-like structure of spherulites in γ-iPP[42]

The melting point of this form is mostly reported from 125 to 150 °C for low molecular weight samples. In the case of pressure crystallized samples, the melting occurs above 150 °C.[25]

1.3.4 Smectic Form

This form is often referred to as smectic and was first mentioned in 1958 by Slichter and Mandell.[46] It is prepared by quenching thin sheets of iPP from the melt into the ice water.

The density of the smectic form has been reported by Natta to be 0.88 g/cm^3.

The interpretation of the structure is still disputed in literature.[21] Generally, it is characterized by an order intermediate between those found in crystalline and in amorphous phases.[46]

1.4 PROPERTIES

Commercial PP is 90–95 % isotactic and has a number average molecular weight of 220 000–700 000 g/mol with molecular weight distribution (Mw/Mn) varied from 2.1 to over 11.

PP is stiffer than polyethylene, having tensile modulus strength of 1 000–1 300 MPa. Its elongation at break is 50–300 % and its impact strength is 0.3–4.3 J. Generally, the melting temperature is 160–171 °C. PP is non-polar hence it is highly resistant to attack by polar chemicals but can swell, soften, or undergo surface cracking in the presence of the liquid hydrocarbons or chlorinated solvents. Strong oxidizing agents such as fuming nitric acid or hot concentrated sulfuric acid can cause swelling and polypropylene degradation. The high dielectric strength and low dielectric constant and dissipation factor of polypropylene make it useful as an insulating material. The presence of tertiary hydrogen on each repeat unit makes it very susceptible to oxidative degradation. As a plastic material PP is mainly used as an injection moulding material.[5, 9]

The experiments comparing α-iPP with β-iPP resulted in lower elastic modulus and yield stress of β-iPP at a given strain rate, but had a higher ultimate tensile strength and strain (Table 1). The impact strength, breaking strain and toughness of β-iPP exceeds that of α-iPP.[47, 48]

Table 1. Static tensile characteristics of α- and β-iPP (Deformation rate=1mm/min) [38]

Property	α-iPP	β-iPP
E-modulus [GPa]	2.0	1.8
Yield stress [MPa]	36.5	29.5
Elongation at yield [%]	~ 12	~ 7
Necking stress [MPa]	27.5	28
Elongation at necking [%]	~ 22	-
Tensile strength [MPa]	39.5	44
Elongation at break [%]	~ 420	~ 480

The Relation Between the Melt Flow Index Value and the Polypropylene Characteristics

The melt flow index (MFI) is the measure of a polymer's ability to flow under certain conditions. It is defined as the weight of polymer in grams flowing

in 10 minutes (g/min) through a capillary of specific diameter and length by a pressure applied via prescribed alternative gravimetric weights for alternative prescribed temperatures. The method is given in ISO 1133.[48]

Melt flow provides an indication of the resin's processability, such as in extrusion or moulding, where it is necessary to soften or melt the polymer.[48]

The value of MFI is adherent to the average molecular weight. The weight-average molecular weight of polypropylene generally ranges from 220 000–700 000 g/mol, with melt flow indexes from less than 0.3 g/10 min to over 1 000 g/10 min. The melt flow index provides an estimate of the average molecular weight of the polymer, in an inverse relationship; high melt flow index indicates a low molecular weight. Viscous materials with low MFI values (<2) are used in extrusion processes such as production of sheets and blow moulding, that require high melt strength. Resins with MFI values of 2–8 are used in film and fiber applications, and materials with MFI values of 8–35 or more are used in extrusion coating, injection moulding of thin-walled parts that requires rapid mould filling, and fiber spinning. The toughness of a grade of polypropylene is directly related to molecular weight: higher molecular weights provide greater toughness. As a result, higher molecular weight polypropylenes have greater impact resistance and elongation and less brittleness, see Table 2. *[9]*

Table 2: Effect of MFI on properties of polypropylene[9]

Property	With Decreasing MFI
Impact Resistance	Increases
Elongation	Increases
Modulus	Decreases
Strength	Decreases
Shear Rheology	Increases
Melt Strength	Increases
Heat Seal Strength	Increases
Heat Distortion Temperature	Decreases
Irradiation Tolerance	Decreases
Haze	Decreases
Solubility	Decreases
Crystallization temperature	Decreases

2. UV-DEGRADATION

Degradation of plastics is defined as an aggregate of irreversible changes of material characteristics caused by chemical, physico-chemical and physical processes, leading to undesirable non-reversible changes of the features of the polymers. Deterioration of polymeric materials is effected by light, weather conditions, temperature, ozone, oxygen, chemical attack or mechanical stress.[50]

The process of the degradation caused by solar radiation, usually ultraviolet radiation (UV) is called UV-degradation or photodegradation. Considering the mechanism and the conditions of the reactions the oxygen takes place indeed, when gear the reactions. That means that in normal conditions when the polymers are used the provisions for the degradation caused by the UV-light and the oxygen together have to be made. This type of degradation is called photooxidative degradation (photooxidation). A lot of polymeric materials are, more or less, sensible to the act of UV radiation. For iPP the UV-degradation is the most considerable type of the degradation.

Composition of the solar radiation reaching the earth's surface is mainly made up of radiation in the visible and infrared areas of the electromagnetic spectrum. Approximately 43 % of solar radiation is in the infrared region and has a wavelength of greater than 700 nm - this radiation does little to most plastics apart from heating the material. Approximately 52 % of solar radiation as in the visible region and has a wavelength of between 400 and 700 nm – this radiation both heats the plastic and can also start photochemical reactions. The last 5 % of the radiation is in the ultraviolet region and has a wavelength of between 290 and 400 nm.[51]

The approximate lower boundary of 290 nm is due to the filtering effect of the ozone layer in the atmosphere blocked by the ozone layer and prevented from reaching the earth's surface. UV-radiation can be classified as near, far or extreme UV but it is also possible to classify UV radiation in terms of UVA, UVB and UVC. Only UVA and UVB ultraviolet rays reach the earth's surface.[51]

Despite the relatively low percentage of UV-radiation present in the solar spectrum, it is a very damaging radiation for plastics because of the high quantum energy content. The bonds between the atoms in many plastics have dissociation energies that are very similar to the quantum energy present in UV-radiation. UV-radiation in the region of 300 to 400 nm is therefore capable of breaking the bonds in the plastic to cause rapid degradation of the basic structure of the plastic. The most damaging UV-wavelength for a specific plastic depends on the bonds present and the maximum degradation therefore occurs at different wavelengths for different types of plastics.[51]

2.1 PHOTOPHYSICS

Visible light, infrared, UV, and γ-rays are each a distinct form of electromagnetic radiation. Each propagate in space as waves of electronic and magnetic fields. Electromagnetic waves carry a discrete amount of energy depending on their frequency, as stated by Planck's Law:

$$E = hf \qquad (1)$$

where E…energy of radiation [J]
f…frequency of radiation [1/s]
h…Planck's constant [J.s].

The frequency of radiation depends on the conditions in which this radiation was formed. With temperature increase, the light spectrum is shifted to the left, meaning that more UV and visible light is emitted (the frequency of radiation depends on conditions of emission, mainly temperature). Table 3 presents the wavelengths and energies of given radiation.

Table 3. Energy of radiation[52]

Type	λ [nm]	Energy [kJ/mol]
UVC	100–280	1196
UVB	280–315	598
UVC	315–400	399
Blue-green	500	239
Red	700	171
Near IR	1000	120
IR	5000	24
Hard X-rays, soft γ-rays	0.05	2.4×10^6
Hard γ-rays	0.005	2.4×10^7

The outcomes of energy absorption by molecules are well demonstrated in Jablonski diagram (Fig. 12). At first electrons in molecule of polymer absorb the radiation energy. Depending on the energy absorbed by the molecule, the electrons are promoted from ground state to higher energy state levels. The absorbed energy is then dissipated either in radiative processes as fluorescence and phosphorescence or in non-radiative processes during which the absorbed energy is converted.

The non-radiateve process, in dependence on the balance of energy available in a particular molecule and the chemical structure of the excited molecule, can lead to cleavage into free radicals, abstraction of hydrogen atom, photosensitization, decomposition with formation of two or more molecules, photodimerization or crosslinking, intramolecular rearrangement, photoisomerization. Which reaction type predominates partly depends on the environment. These primary photochemical reactions are mostly followed by secondary reactions. A mostly reactions with oxygen, ozone and photooxidation are realized.[52]

2.2 UV-DEGRADATION OF POLYPROPYLENE

PP is with respect to the other polymeric materials unstable to weather conditions. PP especially comes under the oxidative degradation initiated by UV-irradiation. The failure shows itself as a brittle fracture resulting from surface embrittlement.[52]

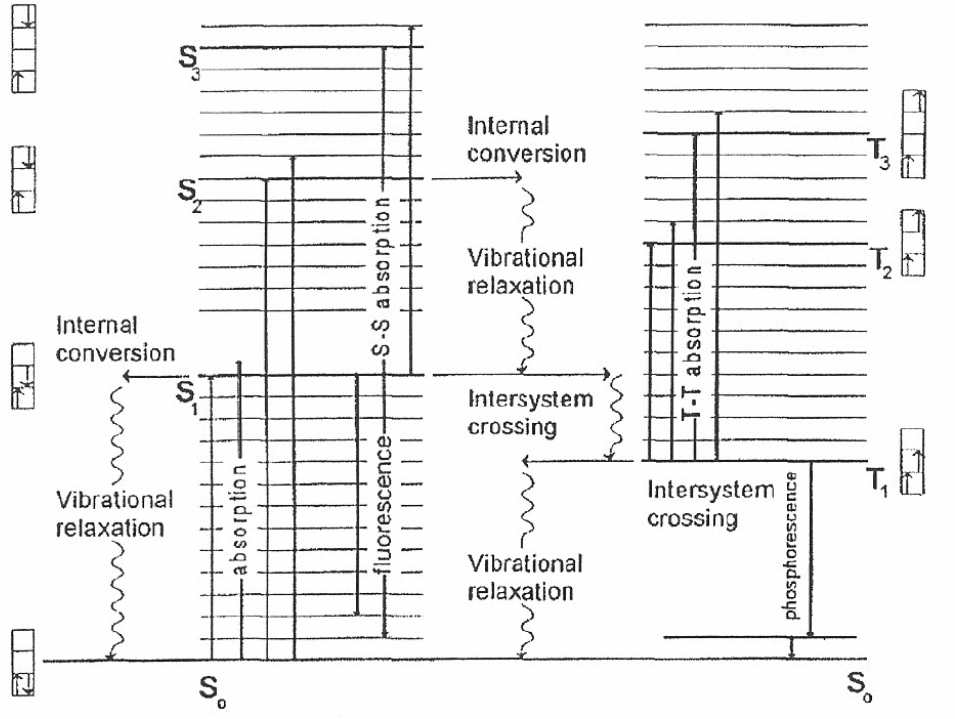

Fig. 12: Jablonski diagram[52]

The reason that the PP is not resistant to the solar radiation is the presence of the tertiary carbons in polypropylene macromolecule which are vulnerable to the oxidative destruction.

The polypropylene itself does not absorb the light above the wavelength 200 nm. The photolysis of the commercial PP by the light of the wavelength about 290 nm is caused by the chromophores, which are developed during the polymerization or the thermal processing. Chromophores are sensitive to the photolysis by the light above the wavelength 300 nm. Greatest changes in the PP are evoked by the spectra from 300 nm to 340 nm. The photodegradation is accelerated by the damp and the warmth. The 10 °C raise of the temperature causes two time quickened photooxidative degradation of PP.[53]

In the natural atmospheric conditions insolating of PP generally causes:[53]

- Embrittlement of the material
- Cracking of the surface (the cracks are oriented across the orientation of the macromolecules; during the exposition the number of the cracks increases, the cracks leak deeper in the material and link)
- The change of the colour (PP gets yellow or brown, over the further ageing the colour gets darker; the colour is changed before any

chemical changes appear in the sample thence it follows that the coloration is caused by the impurities or the presence of the foreign chemical groups in the chain)
- The contraction of the material (length 0.5—1 % and thickness 0.1—0.2 %)
- The chemical changes (growth of the content of the carbonyl and peroxide groups which absorb the solar radiation in field of UV, absorption increase with their quantity)
- The decrease of the mechanical features

2.2.1 The Photooxidative Processes in Polypropylene

Polypropylene weathering involves mainly oxidative degradation, proceeding as a radical reaction with branched kinetic chains. This chain reaction is composed of four main stages: initiation (I), propagation (II), chain branching (III) and termination (IV).[54]

I	$PH + O_2 \rightarrow P^{\cdot} + HO_2^{\cdot}$	(2)
II	$P^{\cdot} + O_2^{\cdot} \rightarrow POO^{\cdot}$	(3)
	$POO^{\cdot} + PH \rightarrow POOH + P^{\cdot}$	(4)
III	$POOH \rightarrow PO^{\cdot} + HO^{\cdot}$	(5)
IV	$2POOH \rightarrow POO^{\cdot} + PO^{\cdot} + H_2O$	(6)

Radicals formed in (III) then re-enter the propagation phase via the following reactions:

$PO^{\cdot} + PH \rightarrow POH + P^{\cdot}$	(7)
$HO^{\cdot} + PH \rightarrow P^{\cdot} + H_2O$	(8)
$P^{\cdot} + P^{\cdot} \rightarrow$ inactive products	(9)
$P^{\cdot} + POO^{\cdot} \rightarrow$ inactive products	(10)
$POO^{\cdot} + POO^{\cdot} \rightarrow$ inactive products	(11)

Initiation is promoted by photon in the UV-part of the solar spectrum and it is caused by collision of a photon with an impurity. Further molecular degradation occurs because the radicals are unstable and may undergo scission or crosslinking reactions. Scission dominates, but both reactions lead to deterioration of the engineering properties of the material.

Hydroperoxides produced by reaction (3) and (4) can be decomposed by UV-radiation with wavelength below 360 nm giving a $PO^{\cdot}$ radical (5) and (6). Hydroperoxide decomposition is central in the degradation of PP. Carbonyl groups are produced during PP oxidation and are themselves photolabile. Aldehyde and keton groups are produced and may influence the subsequent photodegradation behaviour.[54]

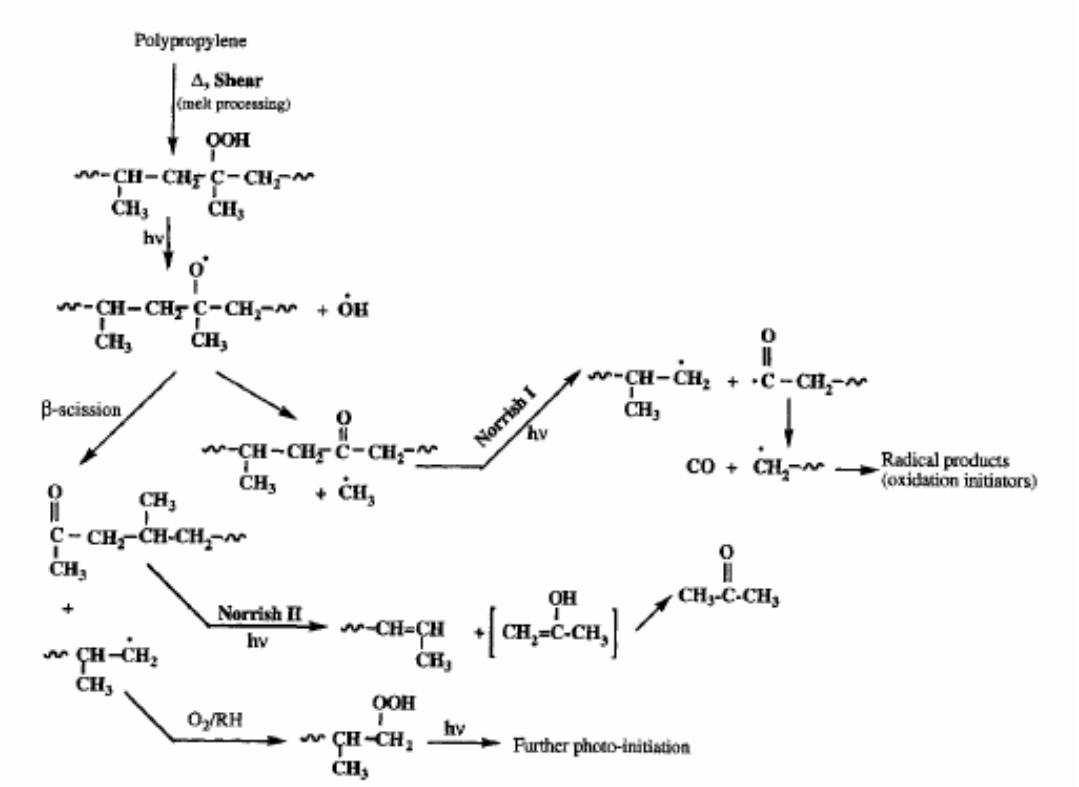

Fig. 13: Polymer hydroperoxidation during processing and further photoinitiation by the hydroperoxides and the derived carbonyl compounds [55]

Polymer hydroperoxidation and further processes leading to the polypropylene degradation are schematically arranged in Fig. 13.

The major failure mode with weathered PP is fracture nucleated in an embrittled surface layer.[54] Generally, photodegradation kinetics in polymer systems basically depends on oxygen permeability through the material and that is why, it is concentrated strongly in the surface zone partly because the UV-intensity is greatest there, but mainly because of the ready supply of oxygen. The reaction near to the surface is so rapid in sunny conditions that oxygen diffusing in from the surface is consumed before it can penetrate far into the polymer and no more oxidation is possible in the interior as long as UV-irradiation continues.[54] The rate of oxidation drops with decreasing oxygen diffusion, following the increase of crystallinity and molecular orientation. This rise of crystallinity, which is called chemicrystallization, is caused by the scission of molecular chains in the amorphous region; released molecular entanglements facilitate additional crystallization in the solid state.[56, 57] Weathered PP often develops tensile residual stresses in the surface as a consequence of the volumetric contraction caused by crystallization, further enhancing its vulnerability to cracking. When the surface is put into the tension cracks form readily in the embrittled layer and often propagate into interior, leading to failure.[54]

If the UV-source is applied only intermittently the oxygen level may recover during the dark periods. The presence of stabilizers has an important effect on the depth-distribution of degradation. Stabilizing system slows the reaction near the surface so much that oxygen diffusion into the interior is possible and the level of degradation there may be higher than in an unstabilized system.[54]

2.2.2 Effect of Morphology on Photodegradation Kinetics

As generally accepted, degradation reactions of semicrystalline polymers proceed predominantly in amorphous regions. Nevertheless, physical factors, such as the arrangement and distribution and the size of crystalline regions, affect the degradation process as well. The major role in determining the properties of these materials plays directly the spherulite size.[58, 59] The higher spherulite size in slow cooled samples in comparison with normal cooled samples makes these specimens particularly vulnerable to the weathering effects due to the expected lower concentration of tie chain molecules.[60]

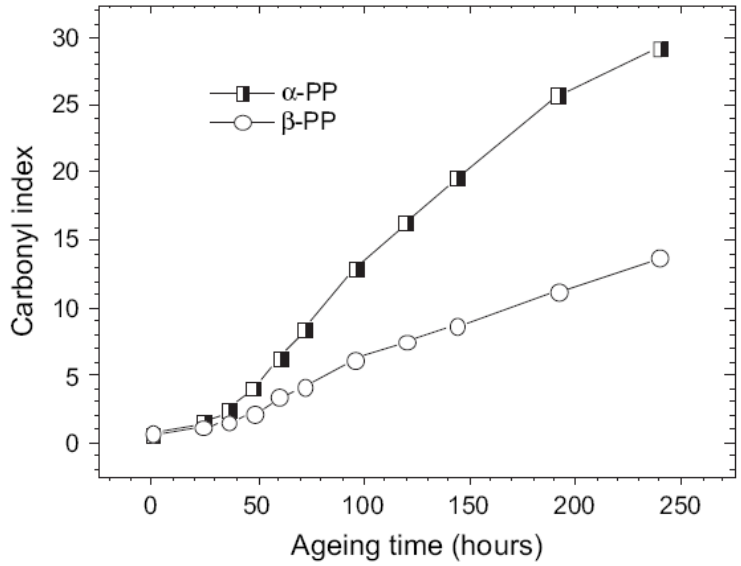

Fig. 14: Effect of UV exposure on molecular degradation of a-iPP and B-iPP[60]

As well as the spherulite size the crystal size is important. If the lamellar thickness of the slow cooled sample is large, as expected, then there will be relatively small number of chain folds available for reaction at the crystal surface. It is expected that the extent of degradation will decrease with the increase in the degree of crystallinity and molecular orientation, following the effects of these parameters on oxygen diffusion. On the other hand, the crystallinity and the molecular orientation determine the mobility of the radicals and therefore reduce the rate of termination, allowing an increase in the propagation of chemical reactions leading to molecule scission, and this effect is opposite to that caused by reduced oxygen mobility.[60]

As is written above, it is accepted, that degradability of semicrystalline polymers is significantly influenced by their morphology.[e.g. 62-64] It was found, that the β-nucleation specifically affects the processes of UV-degradation of isotactic polypropylene. The molecular degradability of β-iPP is lower as compared to α-iPP, reflecting higher opacity of β-iPP for UV-light; the

degradation mechanism, however, is similar for both materials. Fig. 14 shows the molecular degradation of both the neat and β-nucelated polypropylene as a function of ageing time.[16] Molecular degradation is characterized by carbonyl index. The degradation is more pronounced for α-iPP and particularly evident at higher ageing times. It indicates a more intensive molecular degradation of α-iPP.

3. METHODS

3.1 INFRARED SPECTROSCOPY

Infrared (IR) spectroscopy is the subset of spectroscopy that deals with the infrared part of the electromagnetic spectrum. This covers a range of techniques, with the most common type by far being a form of absorption spectroscopy. As with all spectroscopic techniques, it can be used to identify a compound and to investigate the composition of a sample.[65]

The infrared portion of the electromagnetic spectrum is divided into regions: the near-, short-, mid-, long- and far-infrared light (Fig. 15), named for their relation to the visible spectrum. The far-infrared light, (wavenumber approx. 400–10 cm^{-1}) lying adjacent to the microwave region, has low energy and may be used for rotational spectroscopy. The mid-IR light (wavenumber approx. 4 000–400 cm^{-1}) may be used to study the fundamental vibrations and associated rotational-vibational structure, whilst the higher energy near-IR light (wavenumber 14 000–4 000 cm^{-1}) can excite overtone or harmonic vibrations.[65]

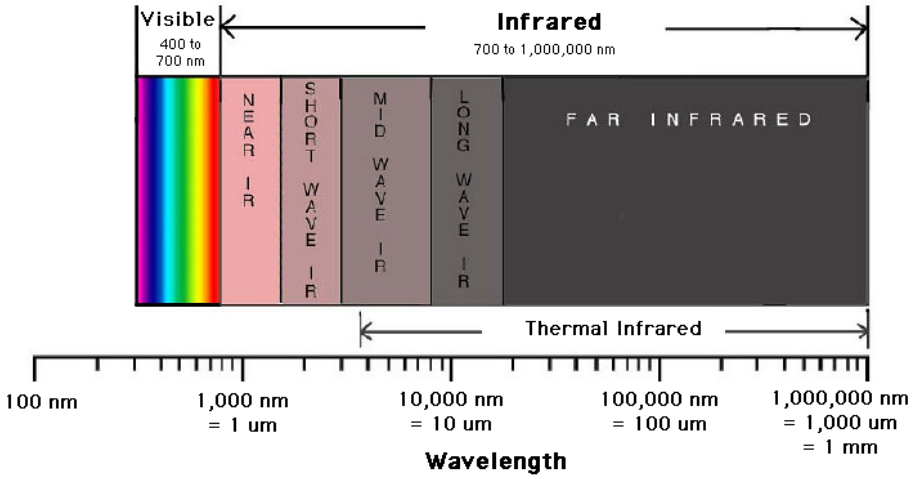

Fig. 15: Infrared spectrum[66]

Infrared spectroscopy works because at temperatures above zero Kelvin all atoms in molecules are in continuous vibration with respect to each other. When the frequency of a specific vibration is equal to the frequency of the IR radiation directed on the molecule, the molecule absorbs the radiation. The resonant frequencies or vibrational frequencies are determined by the shape of the molecular potential energy surfaces, the masses of the atoms and, eventually by the associated vibronic coupling. In order for a vibrational mode in a molecule to be IR active, it must be associated with changes in the permanent dipole. The resonant frequencies can be in a first approach related to the strength of the bond, and the mass of the atoms at either end of it. Thus, the frequency of the vibrations can be associated with a particular bond type (Fig.16).[65, 67]

Simple diatomic molecules have only one bond, which may stretch. More complex molecules may have many bonds, and vibrations can be conjugated, leading to infrared absorptions at characteristic frequencies that may be related to chemical groups.[65]

In order to measure a sample, a beam of infrared light is passed through the sample, and the amount of energy absorbed at each wavelength is recorded. This may be done by scanning through the spectrum with monochromatic beam,

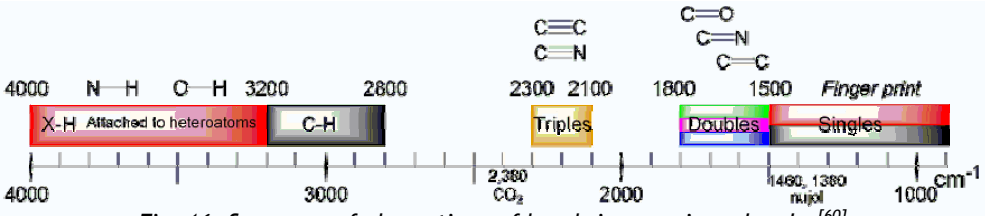

Fig. 16: Summary of absorptions of bonds in organic molecules[60]

which changes in wavelength over time, or by using a Fourier transform instrument (Fourier transform infrared spectroscopy) to measure all wavelengths at once. From this, a transmittance or absorbance spectrum may be plotted, which shows at which wavelengths the sample absorbs the IR, and allows an interpretation of which bonds are present.

From the construction point of view the IR spectrometers can be divided on the dispersive ones with monochromator and Fourier-transform with the Michaelson interferometer.

3.1.1 Dispersive Infrared Spectrometer

A beam of infra-red light is produced and split into two separate beams. One is passed through the sample, the other passed through a reference which is

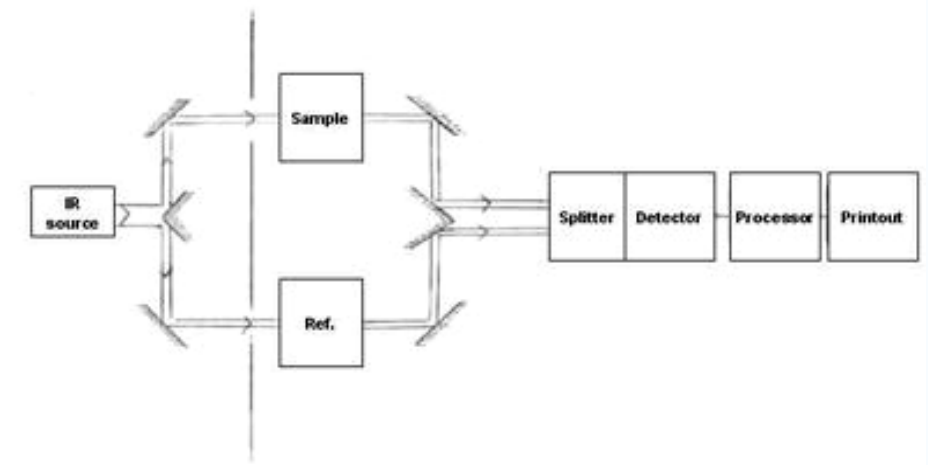

Fig. 17: A typical dispersive infrared spectrometer[65]

often the substance the sample is dissolved in. The beams are both reflected back towards a detector, however first they pass through a splitter which quickly alternates which of the two beams enters the detector. The two signals are then compared and a printout is obtained (Fig. 17).[65]

A reference is used for two reasons:

- prevention of fluctuations in the output of the source affecting the data
- possibility to cancel out the effects of the solvent to be cancelled out (the reference is usually a pure form of the solvent the sample is in)[65]

3.1.2 Fourier Transform Infrared Spectroscopy

Fourier transform infrared (FTIR) spectroscopy is a measurement technique for collecting infrared spectra. The IR light is guided through an interferometer. Fig. 18 shows Michaelson interferometer, where light from the source is split into two beams by a half-silvered mirror, one is reflected off a fixed mirror on the top and one off a fixed mirror on the right. Then the beams are reflected from the half-silvered mirror into the detector. The FTIR is just a Michaelson interferometer but one of the two fully-reflecting mirrors is movable, allowing a variable delay (in the travel-time of the light) to be included in one of the beams. After passing the sample the measured signal is the interferogram. Performing a mathematical Fourier Transform on this signal results in a spectrum identical to that from conventional (dispersive) infrared spectroscopy.[65]

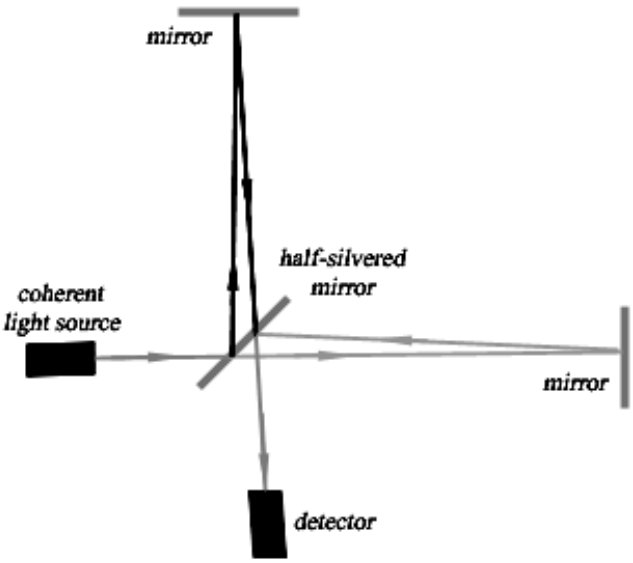

Fig. 18: Michaelson Interferometer[65]

FTIR spectrometers are cheaper than conventional spectrometers and the measurement is faster. This allows multiple samples to be collected and averaged together resulting in an improvement in sensitivity. Because of its various advantages, virtually all modern infrared spectrometers are FTIR instruments.[65]

3.2 X-RAY DIFFRACTION

X-ray scattering is a versatile, non-destructive technique used for the determination of the quality and a quantity of the crystalline structures leading to the statement of the crystalline and amorphous amount phases of the sample and reveals detailed information about the composition of the natural and manufactured materials.

The principle is a diffraction (viewed in Fig.19) of the X-ray radiation beams on the regular structure consequently on the crystal lattice. The crystal diffracts an X-ray beam passing through it to produce beams at specific angles depending on the X-ray wavelength (about 10 nm), the crystal orientation and the structure of the crystal.[68] X-rays are scattered when interacting with the

electrons in the atoms. If the atoms are organized in planes (the matter is crystalline) and the distances between the atoms are of the same magnitude as the wavelength of the X-rays, constructive and destructive interference occurs and a diffraction pattern forms. A diffraction pattern records the X-ray intensity

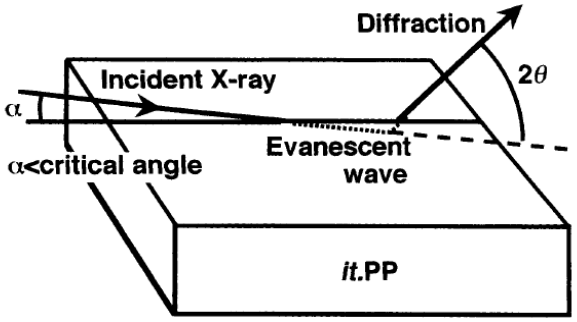

Fig. 19: Schematic illustration of the geometry of X-ray diffraction[69]

as a function of 2θ angle (θ angle is the angle of diffraction and for practical reasons this angle as measured by diffractometer twice – 2θ angle). The distance between similar atomic planes in the interatomic spacing is called the *d*-spacing and measured in nm. The wavelength of the incident X-radiation is symbolized by the Greek letter lambda λ and *n* is an integer.[69] These factors are combined in Braggs law:

$$n\lambda = 2d\sin(\theta) \qquad (12)$$

The position of diffracted peaks provides information about how the atoms are arranged within the crystalline compound (unit cell size or lattice parameter). The intensity information is used to assess the type and nature of atoms.

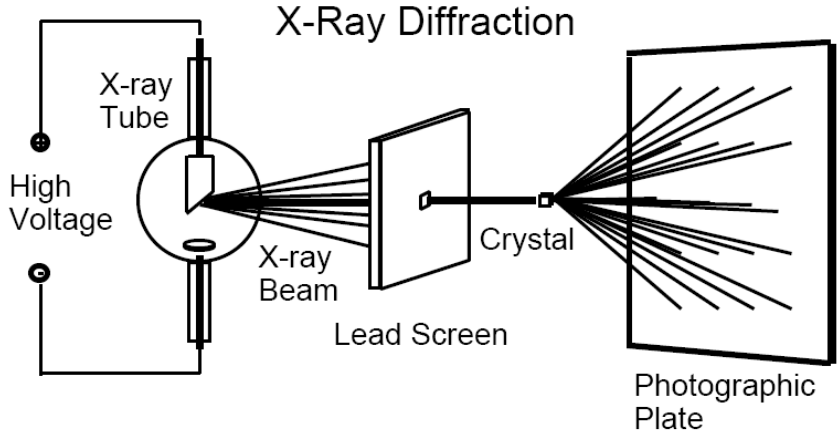

Fig. 20: A scheme of X-ray diffraction[70]

Determination of lattice parameter helps understand extent of solid solution (complete or partial substitution of one element for another, as in some alloys) in a sample. Width of the diffracted peaks is used to determine crystallite size and microstrain in the sample. A scheme of X-ray apparatus is displayed in the Fig. 20.

X-ray diffraction has applications in most fields dealing with solid materials. Areas of application are quite wide and include metals, organic and inorganic compounds.[69]

3.3 OPTICAL MICROSCOPY

The optical microscope is a type of microscope which uses visible light and a system of lenses to magnify images of small samples.

Optical microscopes, through their use of visible wavelengths of light, are the simplest and hence most widely used type of microscope. They use refractive lenses, typically of glass and occasionally of plastic, to focus light into the eye or another light detector. There are a lot of types of optical microscopes but all of them share the same basic components (Fig. 23):

- the eyepiece or ocular - a cylinder containing two or more lenses to bring the image to focus for the eye. The eyepiece is inserted into the top end of the body tube. Eyepieces are interchangeable and many different eyepieces can be inserted with different magnifications.
- the objective lens - a cylinder containing one or more lenses to collect light from the sample. At the lower end of the microscope tube one or more objective lenses are screwed into a circular nose piece which may be rotated to select the required objective lens.
- the stage - a platform below the objective which supports the specimen being viewed.
- the illumination source - below the stage the light is provided and controlled in a variety of ways. At its simplest, daylight is directed via a mirror. Most microscopes, however, have their own controllable light source that is focused through an optical device called a condenser.
- the rigid arm-provide necessary rigidity, possesses the optical assembly

Typical magnification of a light microscope is up to 1 500x with a theoretical resolution of around 0.2 micrometres. The microscopes are limited in their ability to resolve fine details by the properties of light and the refractive materials used to manufacture lenses. Specialized techniques (e.g., scanning confocal microscopy) may exceed this magnification. The resolution *(d)* of the microscope is given by the equation (12):

$$d = \lambda / 2A_N \qquad ([9]12)$$

Usually, a λ of 550 nm is assumed, corresponding to green light. With air as medium, the highest practical A_N (numerical aperture) is 0.95.[75]

Stereo microscope

The stereo or dissecting microscope is designed differently than the classical optical microscope and serves a different purpose. It uses two separate optical paths with two objectives and two eyepieces to provide slightly different viewing angles to the left and right eyes. In this way it produces a three-dimensional (3-D) visualization of the sample being examined.[75]

The stereo microscope is often used to study the surfaces of solid specimens or to carry out close work such as sorting, dissection and the like.

Great working distance and depth of field here are important qualities for this type of microscope. Both qualities are inversely correlated with resolution: the higher the resolution (i.e. the shorter the distance at which two adjacent points can be distinguished as separate), the smaller the depth of field and working distance. A stereo microscope has a useful magnification up to 100×. The resolution is maximally in the order of an average 10× objective in a compound microscope, and often much lower.[75]

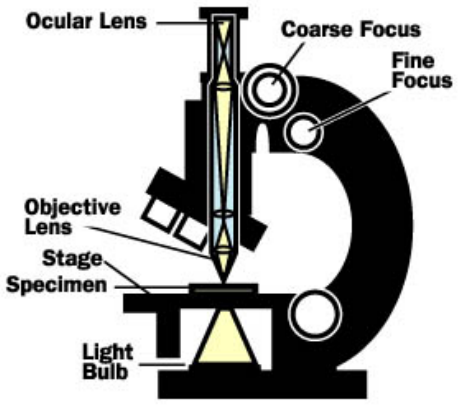

Fig. 21: Optical microscope[76]

Other microscopes which use electromagnetic wavelengths not visible to the human eye are often called optical microscopes. The most common of these, due to its high resolution yet no requirement for a vacuum like electron microscopes, is the X-ray microscope.[75]

3.4 DIFFERENTIAL SCANNING CALORIMETRY

Differential scanning calorimetry (DSC) is a thermoanalytical technique in which the difference in the amount of heat required to increase the temperature of a sample and reference are measured as a function of temperature. Both the sample and reference are maintained at very nearly the same temperature throughout the experiment. Generally, the temperature program for a DSC analysis is designed such that the sample holder temperature increases linearly as a function of time. The reference sample should have a well-defined heat capacity over the range of temperatures to be scanned.[71-73]

The basic principle underlying this technique is that, when the sample undergoes a physical transformation such as phase transitions, more (or less) heat will need to flow to it than the reference to maintain both at the same temperature. Whether more or less heat must flow to the sample depends on whether the process is exothermic or endothermic. For example, as a solid sample melts to a liquid it will require more heat flowing to the sample to increase its temperature at the same rate as the reference. This is due to the absorption of heat by the sample as it undergoes the endothermic phase transition from solid to liquid. Likewise, as the sample undergoes exothermic processes (such as crystallization) less heat is required to raise the sample temperature.[71-73]

Differential scanning calorimeters are able to measure the amount of energy absorbed or released during such transitions. DSC may also be used to

observe more subtle phase changes, such as glass transitions. DSC is widely usedin industrial settings as a quality control instrument due to its applicability in evaluating sample purity and for studying polymer curing.[71-73]

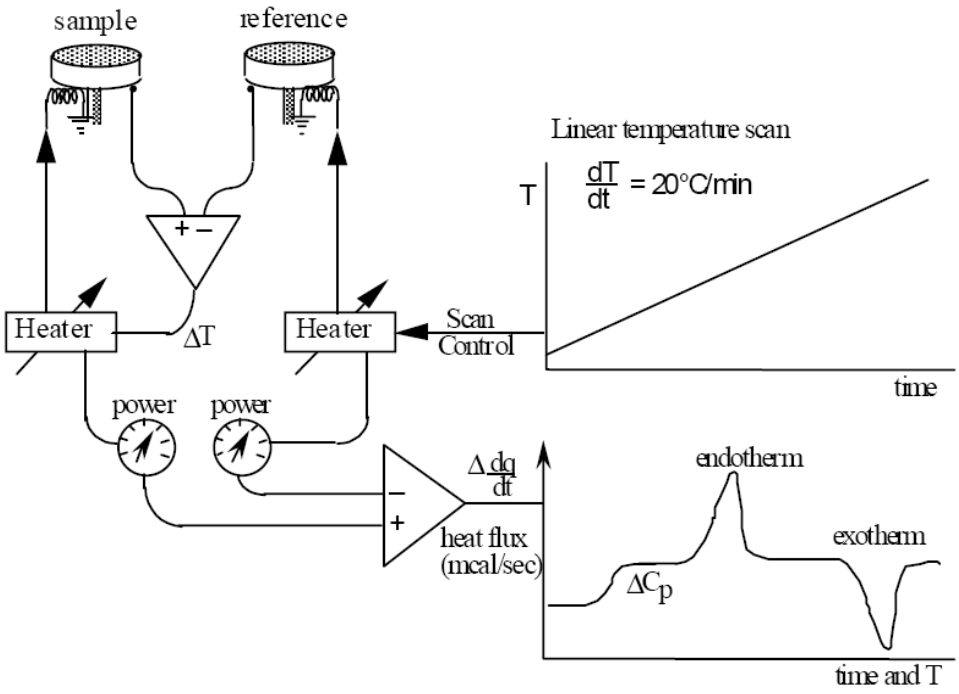

Fig. 22: The simplified model of DSC with linear temperature scan rate. The triangles are amplifiers to determinate the difference in two input signals.[74]

A typical differential scanning calorimeter (simplified model is shown in Fig. 22) consists of two sealed pans: a sample pan and a reference pan (which is generally an empty sample pan). These pans are often covered by or composed of aluminum, which acts as a radiation shield.[71] The two pans are heated, or cooled, uniformly while the heat flow difference between the two is monitored. This can be done at a constant temperature (isothermally), but is more commonly done by changing the temperature at a constant rate.[71] Since the DSC is at constant pressure, heat flow is equivalent to enthalpy changes.[74]

There are two main types of differential scanning calorimeters: heat-flux DSC and power-compensation DSC. In a heat-flux calorimeter, heat is transferred to the sample and reference through a disk made of the alloy constantan or in some cases, silver. The heat transported to the sample and reference is controlled while the instrument monitors the temperature difference between them.[71-73]

In power-compensated calorimeters, separate heaters are used for the sample and reference. This is the classic DSC design. Both the sample and reference are sustained at the same temperature while monitoring the electrical power used by their heaters. The heating elements are kept very small (weighing about 1 gram) in order to ensure that heating, cooling, and thermal equilibration can occur as quickly as possible. The sample and reference are located above their respective heaters, and the temperatures are monitored using electronic temperature sensors located just beneath the samples.[71-73]

The result of a DSC experiment is a heating or cooling curve (Fig. 23). This curve can be used to calculate enthalpies of transitions. This is done by integrating the peak corresponding to a given transition.

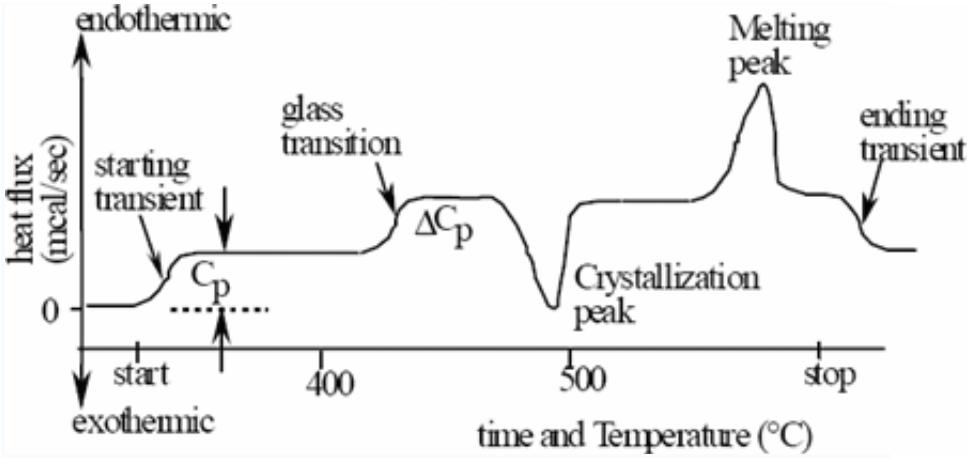

Fig. 23: A schematic DSC curve demonstrating the appearance of several common features[74]

II. EXPERIMENTAL

4. MATERIALS

4.1 POLYPROPYLENES

The basic materials used for the experiments were various types of isotactic polypropylene manufactured by Borealis, Vienna, Austria. In Particular, these materials differ in their MFI values. The homopolymers and some of their characteristics are listed in Table 4.

Table 4: Characteristics of iPPs Borealis

Materials	Melt flow index (230/2.16) [g/10min] ISO 1133	Density [kg/m^3] ISO 1183	Characteristics	Melting temperature [°C] ISO 3146
BE50	0.3	905	high molecular weight low melt flow high stiffness high heat distortion temperature high resistance to thermal ageing	unlisted by producer
HB205TF	1.0	905	low melt flow very good processability and melt stability very good stiffness and impact balance very good organoleptic properties	162-165
HF136MO	20.0	908	good combination of mechanical and flow properties narrow molecular weight distribution	unlisted by producer
HK060AE	125.0	905	low viscosity	unlisted by producer
HL612FB	1200.0	unlisted by producer	narrow molecular weight distribution easy processability optical product consistency very high flow	156-160

For the purpose of the study two sets of materials were used. The first set covers above mentioned neat materials. Another set consists of the same polypropylenes nucleated by a 0.03 wt.% of commercial β-nucleating agent.

4.2 NUCLEATING AGENT

In order to prepare teh β-iPP, a specific β-nucleating agent NJ Star NU 100 (NU 100), produced by Rika International, Japan, was used. The nucleator is based on N,N´-dicyclohexylnaphthalene-2,6-dicarboxamide; its chemical formula model is shown in Fig. 24.

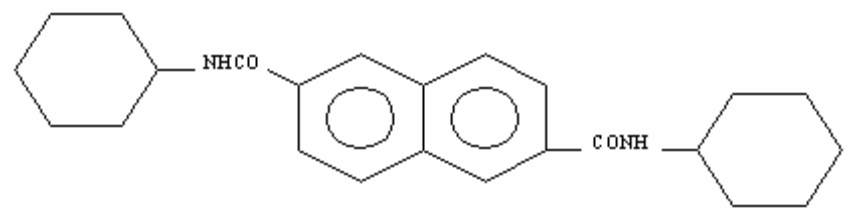

Fig.24: The chemical formula of NJ Star NU 100[79]

5. SAMPLE PREPARATION

Nucleating agent NU 100 was mannualy immixed into iPP pellets and the blends were subsequently processed using twin-screw extruder. The description of blend preparations is described in detail by Lenka Chvatalova (*On Efficiency of specific nucleation in polypropylene*).[77]

Specimens were prepared by compression-moulding. The parameters of processing were set equally. The polypropylene pellets were placed into the template between metal plates and pressed at 230 °C for 6 minutes than cooled at the room temperature. The duration of cooling was 4 minutes. The proportion of the rectangular template was 12.5x6x0.03 cm.

The samples for infrared spectroscopy and X-ray diffraction were carried by aluminium frame to adhere sample throughout on same possition when being measured.

The samples for DSC measurements were taken from UV-irradiated specimens. The samples of weight of approx. 10 mg were put into the aluminium pans by tweezer and subsequently sealed.

6. ANALYZING METHODS AND DEVICES

6.1 UV-EXPOSURE

The specimens were irradiated in SEPAP 12.24 SAIREM ET MPC at 60±2 °C. The SEPAP is equipped with four mercury vapour arc lamps (400 W) with borosilicate envelop emit intense light in the wavelenght range between 290 and 450 nm.

The air flow is produced by two fans resulting homogenous temperature distribution on the sample surface.

During the irradiation the samples were carried in aluminium frames and the exposure was applied for: 0, 24, 36, 48, 60, 72, 96, 120, 144, 192 and 240 hours.

6.2 INFRARED SPECTROSCOPY

The transmission FTIR spectroscopy analysis was (Nicolet, Impact 400) applied to determine chemical changes of the sample in the whole mid-infrared spectrum (4 000−500 cm^{-1}).

This method was employed to analyze the amount of occurred carbonyl groups which characterize the extent of damage caused by UV-irradiation.

In infrared spectra the carbonyl groups are expressed as a peak in the region of 1 700 to 1 800 cm^{-1}. The absorption bands in this region are generally ascribed to carbonyl by-products as convolutions of carboxylic acids, ketones, peresters and lactones.[78, 79]

The amount of carbonyl groups, consequently the molecular degradation is expressed by carbonyl index. Carbonyl index is calculated as the area of the carbonyl absorbtion bands related to the area of a reference band (2 700 to 2 750 cm^{-1}).

6.3 X-RAY DIFFRACTION

The evolution of the crystalline structure of samples during the irradiation was mapped by XPERT-PRO diffractometer. The intended wavelength was $K_\alpha 1$ (0.1540598 nm) and X-ray tube anode was made of copper.. Nickel filter of thickness 0.02 mm was used.

The proportions of the β-form in the samples were calculated from X-ray diffractograms according to Turner-Jones et al. as follows:

$$k\ value = \frac{H_\beta}{H_{\alpha 1} + H_{\alpha 2} + H_{\alpha 3} + H_\beta} \qquad (A),$$

where $H_{\alpha 1}$, $H_{\alpha 2}$, $H_{\alpha 3}$ are the intensities of α-diffraction peaks corresponding to angles 2θ = 14.2°; 17° and 18.8°, respectively, and H_{β} is the intensity of the β-diffraction peak at 2θ = 16.2°. The *k value* approximately gives the relative content of β-phase in the sample. The ratio of the integral intensities diffracted by a crystalline part (I_c) and total integral intensities (I) was used to determine crystallinity ($\chi = \frac{I_c}{I}$).

6.4 POLARIZED LIGHT MICROSCOPY

The surfaces of the degraded materials were surveyed by Stereo microscope ZEISS Stemi 2000-C. The eyepieces may provide magnification form 1.95x to 250x.

6.5 DIFFERENTIAL SCANNING CALORIMETRY

To study the thermal behaviour of irradiated samples the Mettler Toledo DSC 30 was employed. The initial temperature was set up to 25 °and using the temperature rate 10 °C/min the samples were heated to 220 °C, than cooled to 90 °C and subsequently again heated to 190 °C. The temperature was held at all outer values for five minutes. This cycle was applicated to all samples.

III. RESULTS AND DISCUSSION

7. INFRARED SPECTROSCOPY

The results of infrared spectroscopy exhibits the growth of carbonyl index with the irradiation time for both neat polypropylenes and β-nucleated polypropylenes (see Figs. 25 and 26). However, the increasing trend is more pronounced for neat polypropylene, especially at higher ageing times. This experimental finding proves the lower sensitivity of β-nucleated polypropylene to UV-light.[61] It has been already reported that the high UV-stability of b-nucelated polypropylene is caused by its significantly higher haze as compared to neat polypropylene. [61]

Generally, two steps of carbonyl index evolution can be distinguished. First, an induction period where the slope of the curve is small occurs. Second, after the induction period the slope of the curves dramatically increases. The induction period of each neat polypropylene is approx. 48 hours while that of β-nucleated polypropylenes is difficult to recognize. The carbonyl index of β-nucleated polypropylenes increases more gradually as mentioned above, thus, no distinct induction period is observed.

Melt flow index of the materials does not unambiguosly influence the carbonyl index, the curves are very similar. However, some slight deviations can be observed. The carbonyl index of polypropylene with MFI=0.3 rises markedly at the beginning of irradiation as compared to the others materials. After prolonged irradiation time (144 hours and more), the carbonyl index of such material is exceeded by some of the polypropylenes with higher MFR. This is observed for both neat and nucleated materials. Thus, it can be pressumed that the polypropylene with long molecular chains is more sensitive to carbonyl groups development at short time irradiation as compared to others polypropylenes under the study.

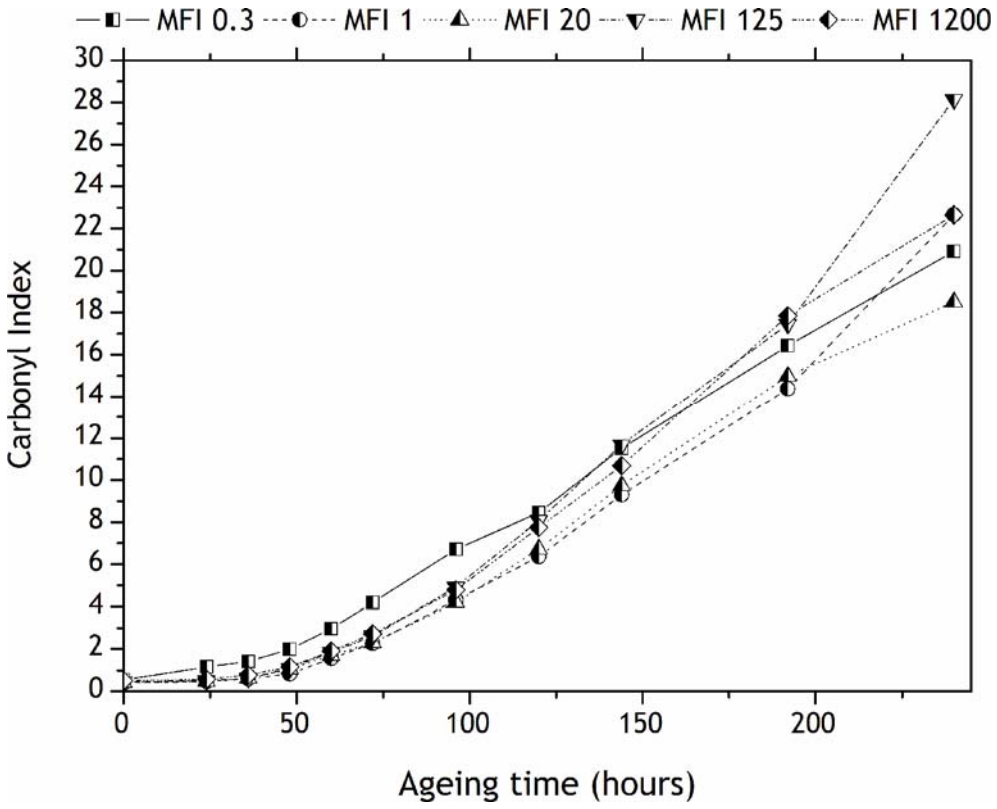

Fig. 25: The effect of UV-irradiation on amount of formated carbonyl groups for neat polypropylene samples

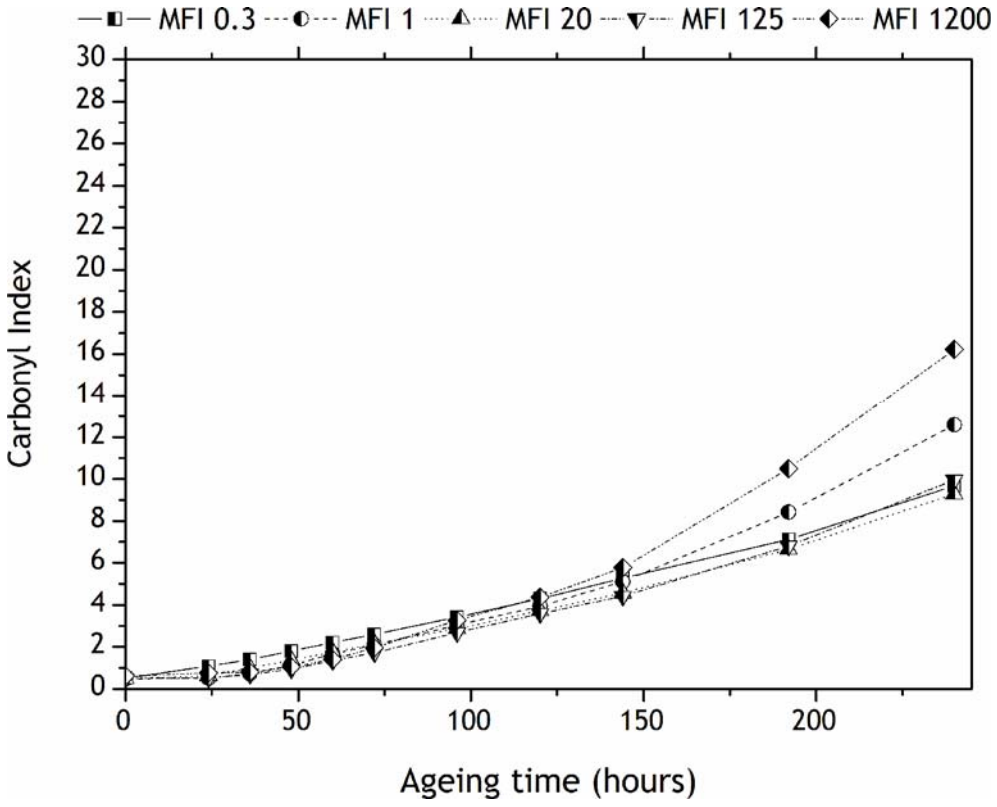

Fig. 26: The effect of UV-irradiation on amount of formated carbonyl groups for β-nucleated polypropylene

8. X-RAY DIFFRACTION

Wide-angle X-ray scattering was employed to observe the evolution of morphology upon UV-irradiation. The X-ray diffractograms of the polypropylenes are shown in Figs. 27-36 and evaluated data are listed in Table A.

As for neat polypropylenes, typical reflections for α-form at angles 2θ=14.2°, 17°and 18.8° can be observed (see Figs. 27-31). In the case of neat iPP of MFI=0.3 also very small reflection at 2θ =16.2° indicating the presence of β-form can be seen. The corresponding K-value of this material is approx. 0.04 and does not change with UV-exposure time. Nevertheless, the presence of β-form is not detected in remaining neat polypropylenes. Thus, it can be derived from these results that long polymer chains support the crystallization into β-form of isotactic polypropylene.

The evolution of diffractograms of all neat polypropylenes under the study upon UV-exposure does not show an uniform trend. The intensity of reflection at angle 14.2 and 17 ° changes during exposure, however, not monotonically. The intensity of other reflections remains virtually unchanged within all exposure.

In the case of β-nucleated polypropylenes the diffractograms show the predominant presence of β-form (see Figs. 32-36). Indeed, the reflection at angle 2θ=16.2° typical for β-form diminates in each diffractogram. The corresponding K-value indicates the amount of β-form of approx 92 % in all the polypropylenes. The K-values of specimens with MFI=0.3 and 1 are slightly lower as compared to polypropylenes with high MFI (see Table A).

The evolution of diffractograms of β-nucleated polypropylenes is not monotonic corresponds to that ofcorresponding to neat polypropylenes. The intensity of β-diffraction peak does not change significantly except of same deviations.

From all diffractogram patterns the crystallinity and β-form contents were calculated (see Table A). The evolution of these characteristics upon UV-exposure is plotted in Figs. 37-38. The results show that the general trend is slightly increasing crystallinity with increasing UV-exposure. The rise of crystallinity can be explained by the process of chemi-crystallization. The chemi-crystallization is caused by the scissions of molecular chains in the amorphous region and, consequently released molecular entanglements facilitate additional crystallization in the solid state.[56, 57] The K-value of β-nucleated polypropylenes remains virtually unchanged within whole UV-exposure period.

Respecting MFI of the material the crystallinity varies from sample to sample. Its values for neat polypropylenes range about 50 % while for β-nucleated polypropylenes the crystallinity reach slightly higher values.

No unambiguos influence of MFI on the crystallinity and its evolution upon UV-irradiation can be derived from the study. Neither the singinicant effect of MFI on b-phase content in the polypropylene is observed, as hase been already published in Master Thesis of Lenka Chvátalová. [77]

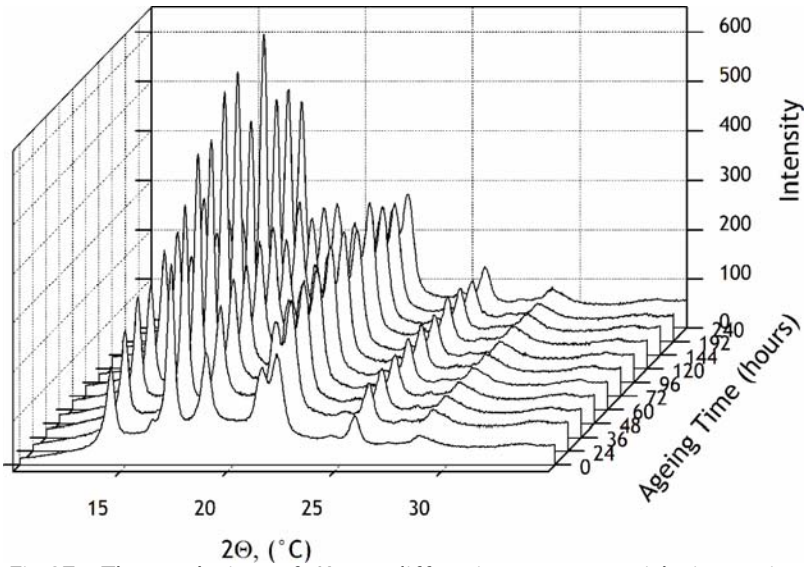

Fig.27: The evolution of X-ray diffraction pattern with increasing exposure time for neat iPP, MFI=0.03

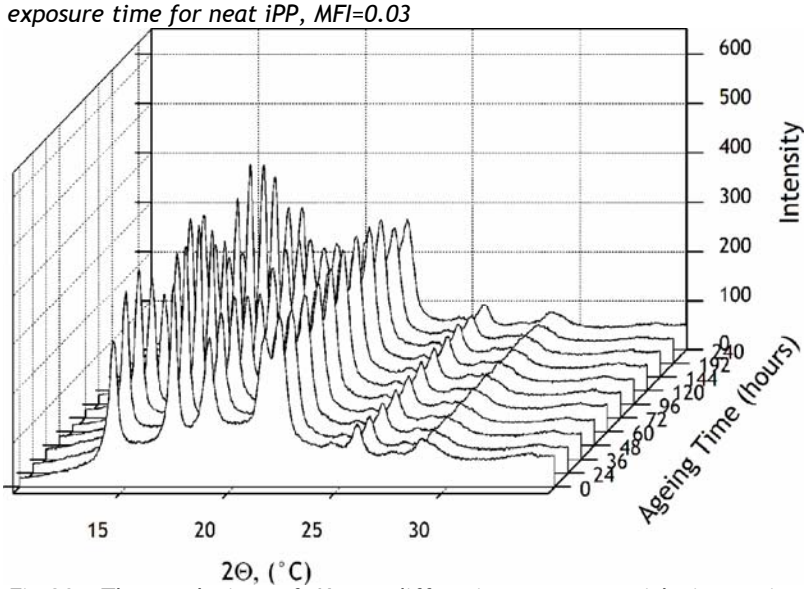

Fig.28: The evolution of X-ray diffraction pattern with increasing exposure time for neat iPP, MFI=1

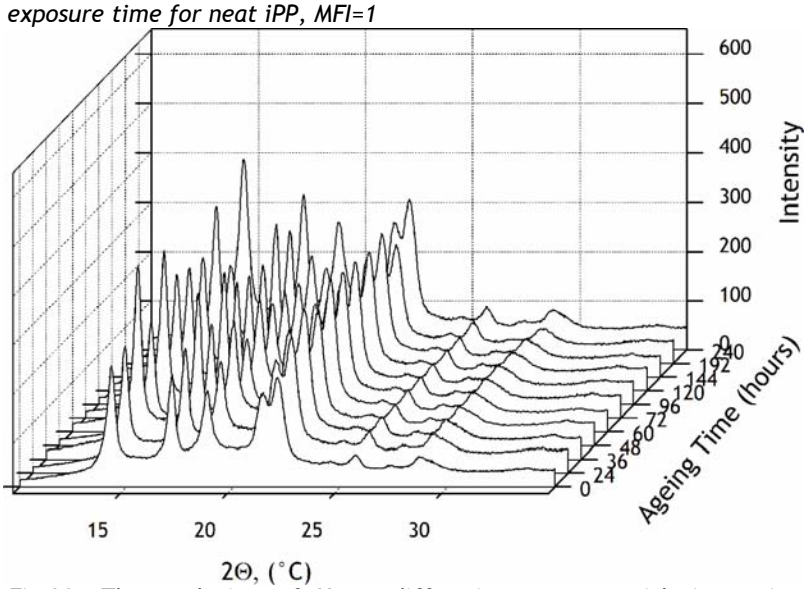

Fig.29: The evolution of X-ray diffraction pattern with increasing exposure time for neat iPP, MFI=20

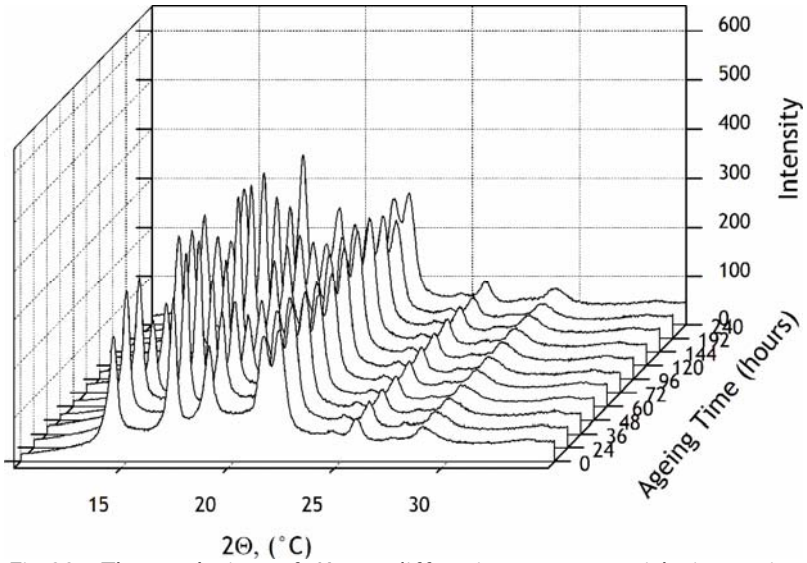

Fig.30: The evolution of X-ray diffraction pattern with increasing exposure time for neat iPP, MFI=125

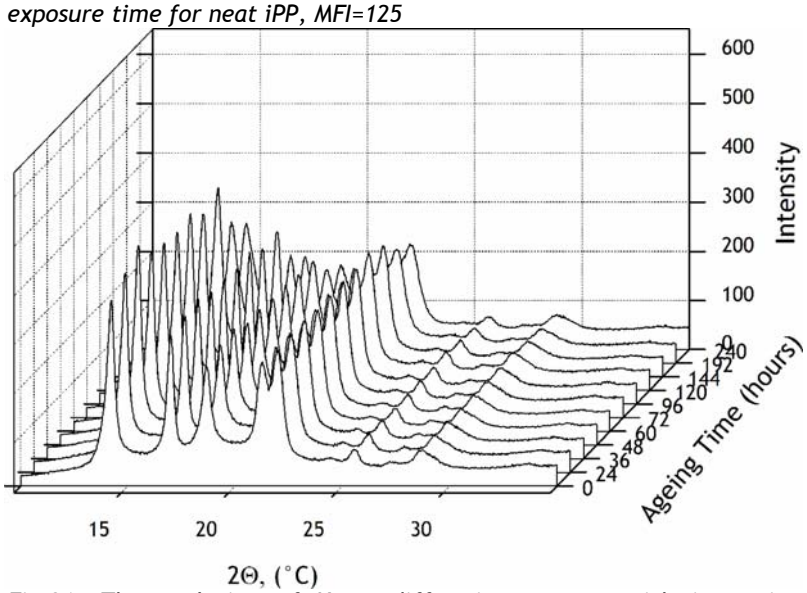

Fig.31: The evolution of X-ray diffraction pattern with increasing exposure time for neat iPP, MFI=1200

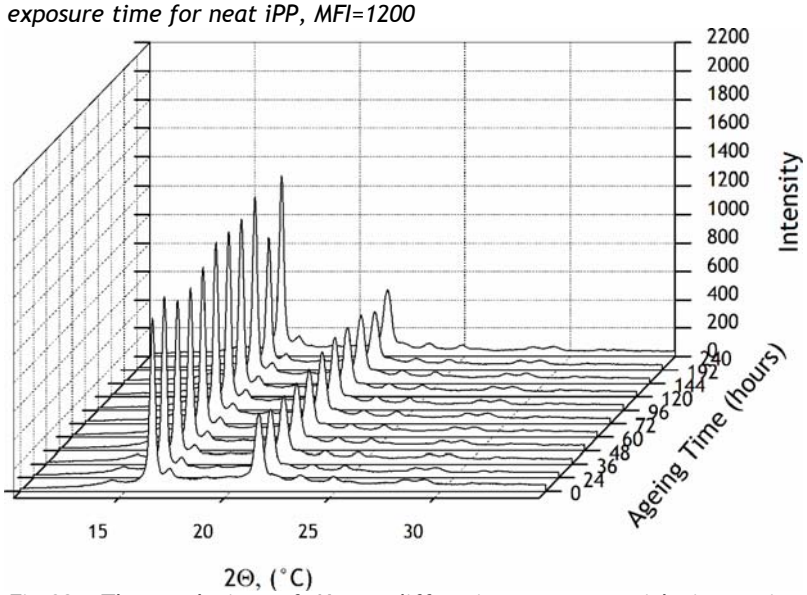

Fig.32: The evolution of X-ray diffraction pattern with increasing exposure time for β-nucleated iPP, MFI=0.03

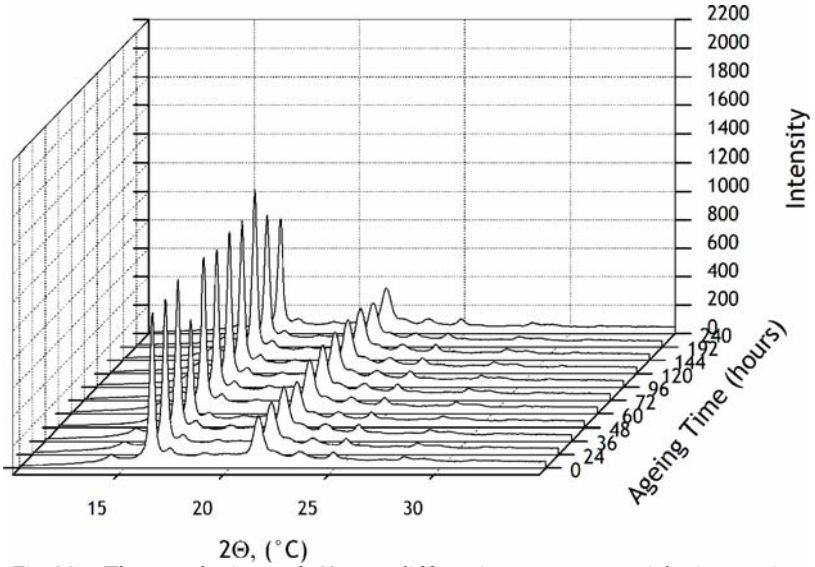

Fig.33: The evolution of X-ray diffraction pattern with increasing exposure time for β-nucleated iPP, MFI=1

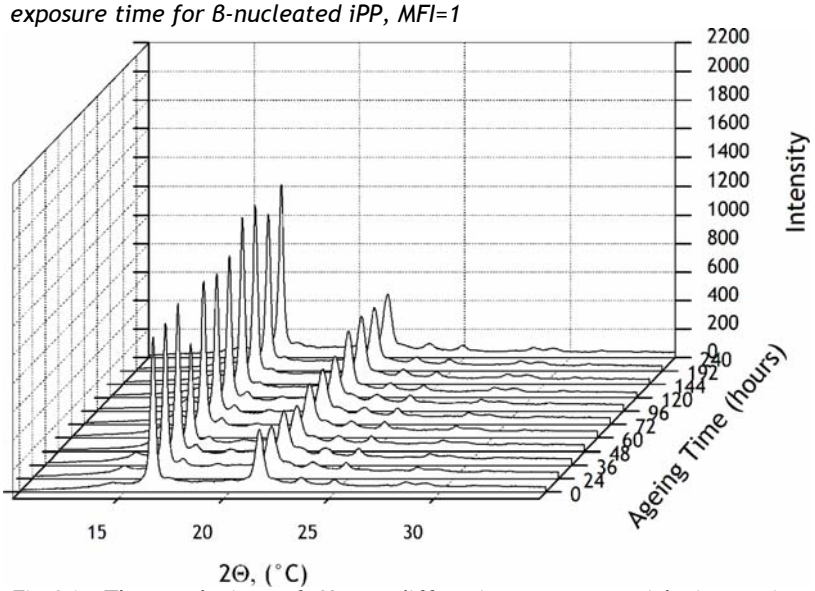

Fig.34: The evolution of X-ray diffraction pattern with increasing exposure time for neat iPP, MFI=20 β-nucleated

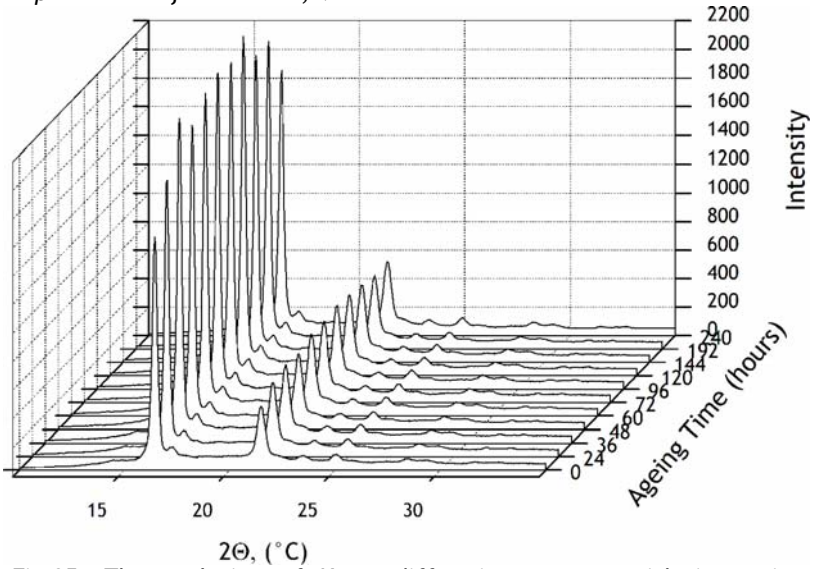

Fig.35: The evolution of X-ray diffraction pattern with increasing exposure time for β-nucleated iPP, MFI=125

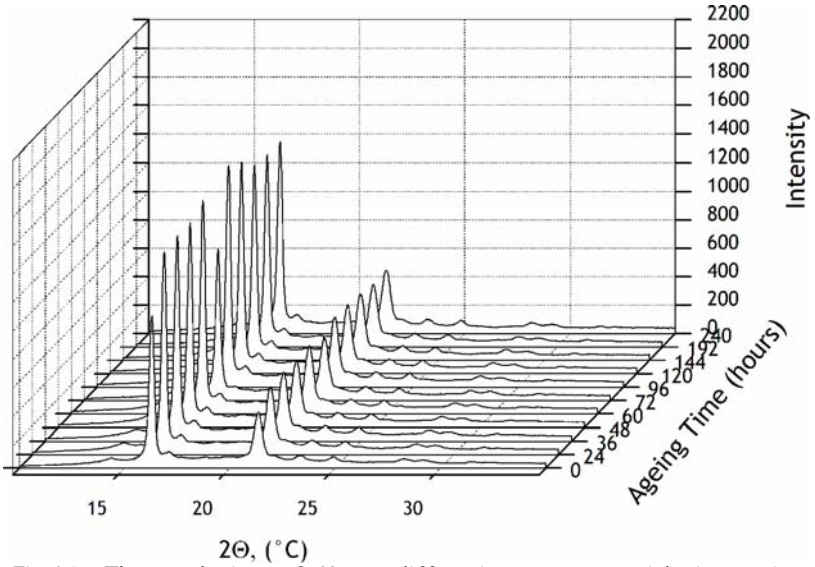

Fig.36: The evolution of X-ray diffraction pattern with increasing exposure time for β-nucleated iPP, MFI=1200

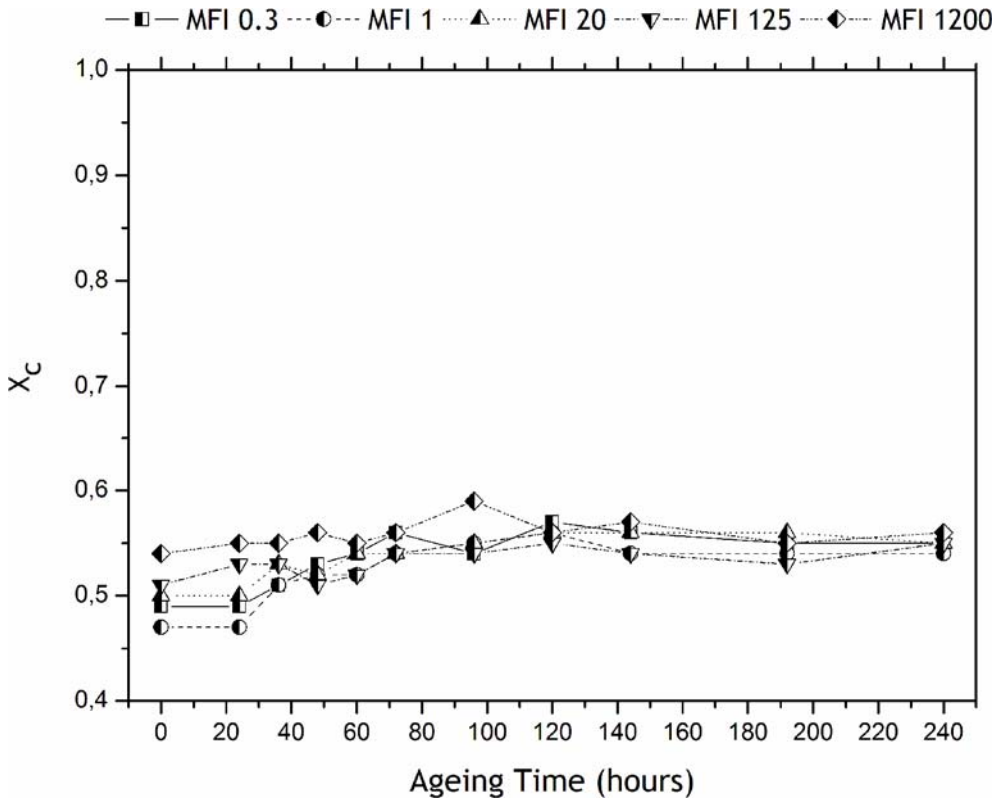

Fig.37: The dependence of crystallinity on UV-exposure time of neat polypropylenes.

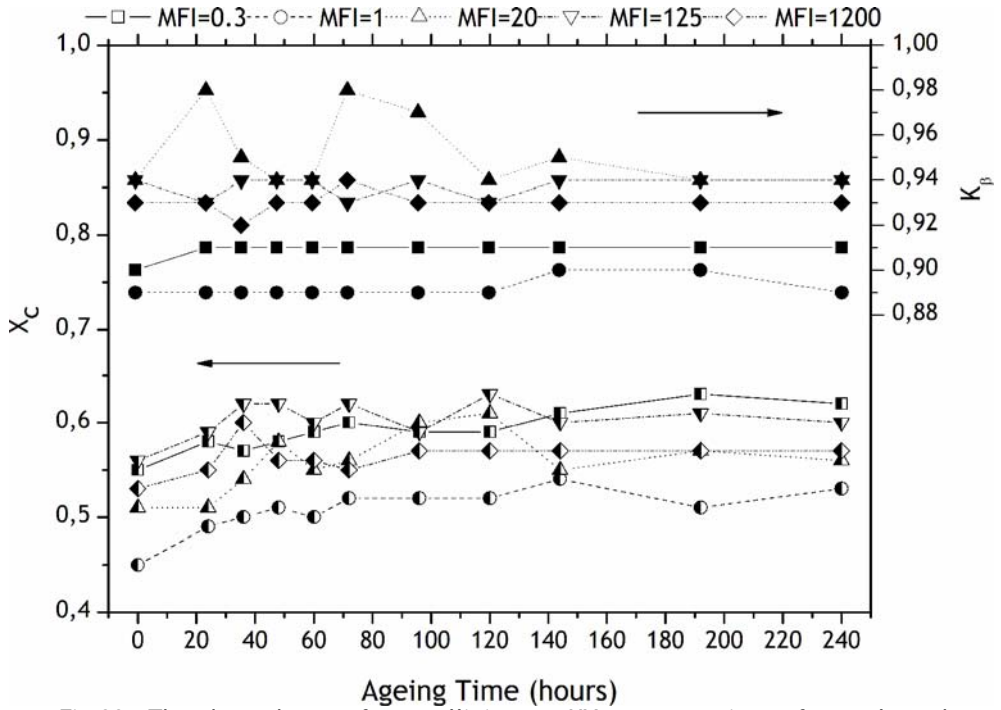

Fig.38: The dependence of crystallinity on UV-exposure time of β-nucleated polypropylenes

9. OPTICAL MICROSCOPY

The micrographs from stereomicroscope display the differences between the surfaces of exposed and unexposed samples, see Figs. 39-48. It can be observed that the different morphology of neat and β-nucleated polypropylene significantly influences the quality of the surfaces after UV-exposure.

The surface of all unexposed samples (Fig. 39a)-48a)) is smooth without the observation of any cracks. The surface of the nucleated samples appears to be more clear and compact since defects are not observed.

Generally, the cracks of the surface are introduced after the UV-exposure. Indeed, the surface of UV-irradiated neat polypropylenes show deap and distant cracks indipendently on the MFI of the material (Fig. 39b)-43b)). Only the polypropylene with MFI=1 seems to embodies the most pronounced cracks. However, this appearance can be evoked by better focalization of corresponding micrograph.

The cracks of the nucleated samples (Fig. 44b)-48b)) are significantly different as compared to neat polypropylenes. They are subtile and form fine network. It correlates to smaller spherulitic size in β-nucleated samples. It can be also seen form the micrographs that the density of crack network increases with increasing MFI of the material.

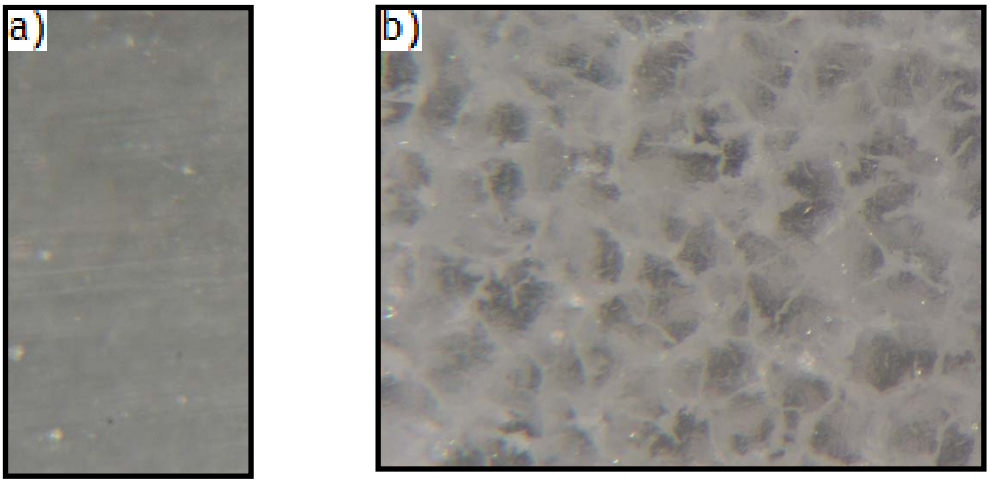

Fig.39: The micrographs of the neat iPP of MFI=0.3, a) unexposed, b) 240 hours exposed sample

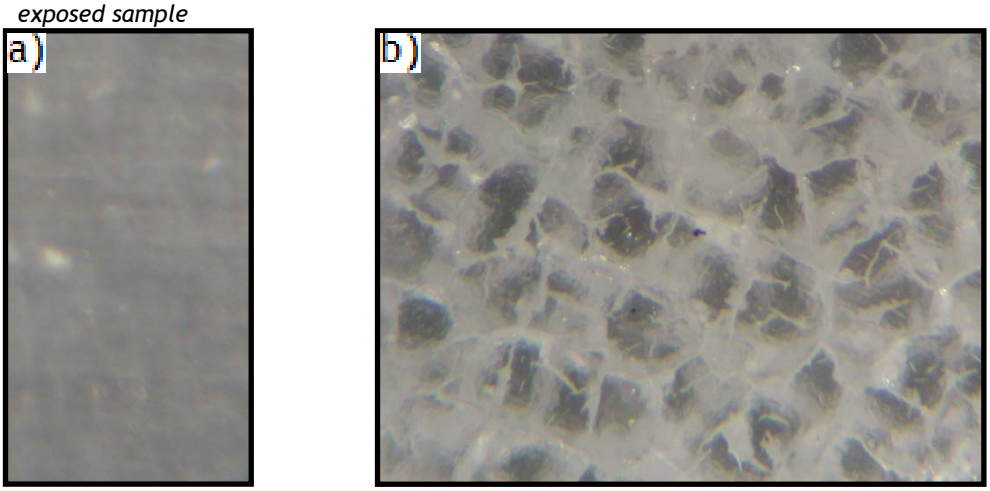

Fig.40: The micrographs of the neat iPP of MFI=1, a) unexposed, b) 240 hours exposed sample

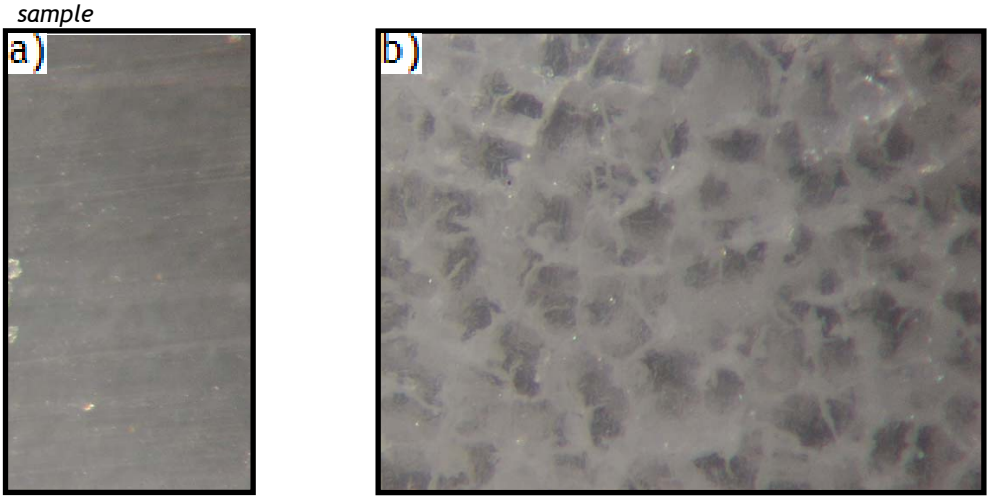

Fig.41: The micrographs of the neat iPP of MFI=20, a) unexposed, b) 240 hours exposed sample

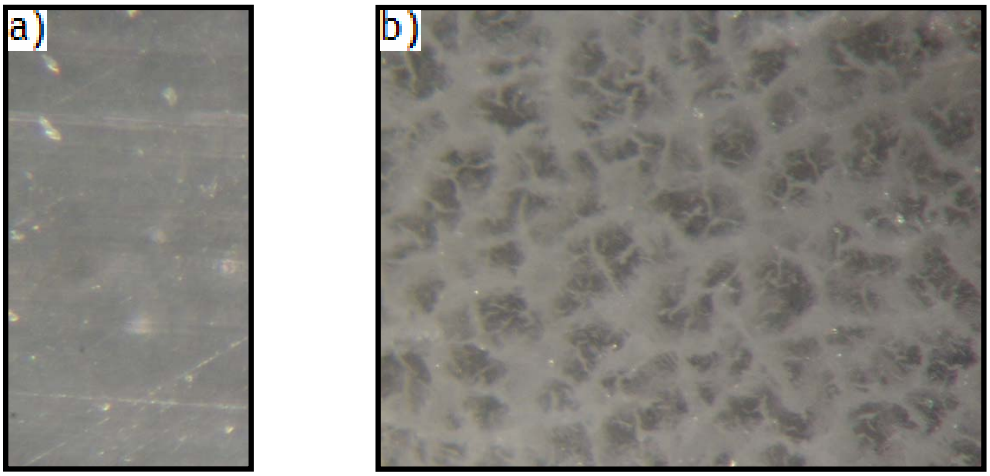

Fig.42: The micrographs of the neat iPP of MFI=125, a) unexposed, b) 240 hours exposed sample

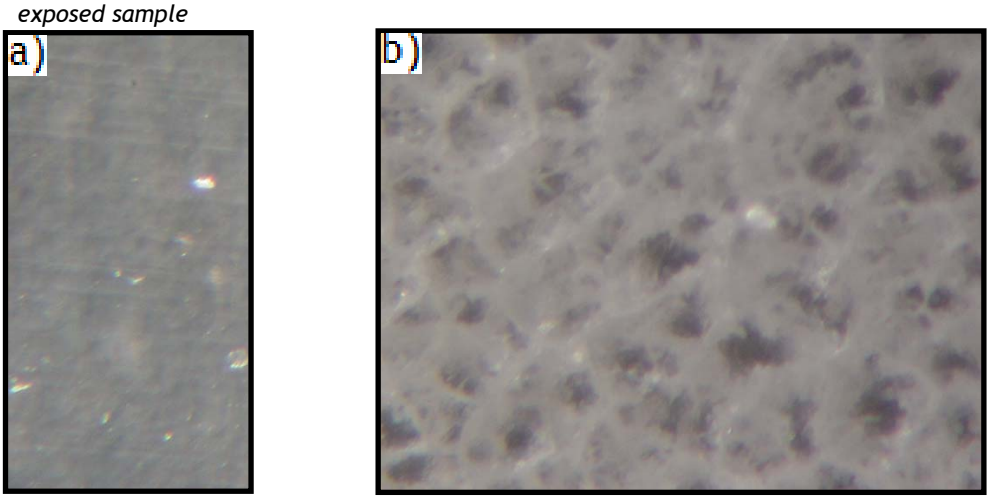

Fig.43: The micrograph of the neat iPP of MFI=1200, a) unexposed, b) 240 hours exposed sample

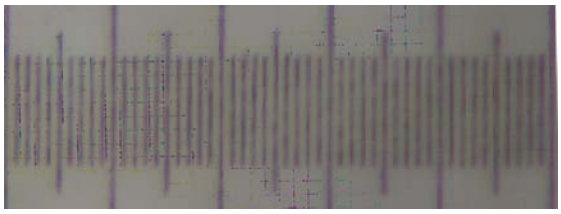

0.5mm

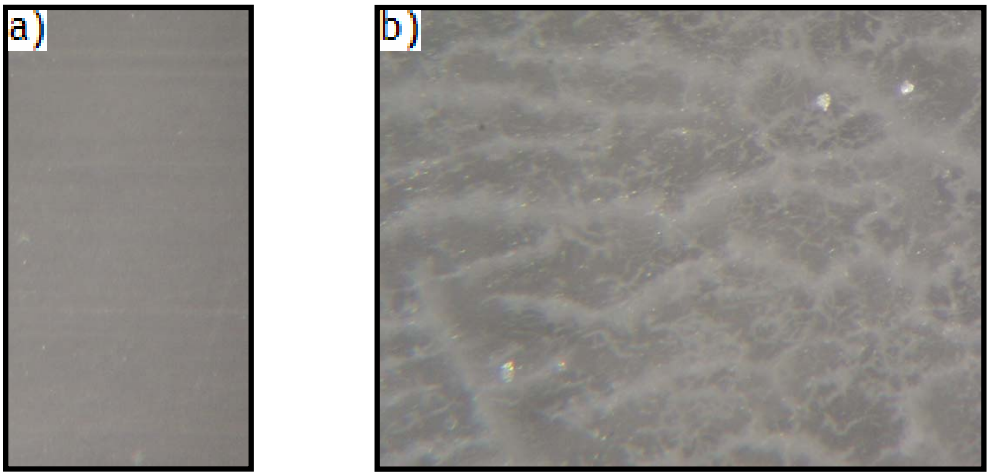

Fig.44: The micrograph of the β-nucleated iPP of MFI=0.3, a) unexposed, b) 240 hours exposed sample

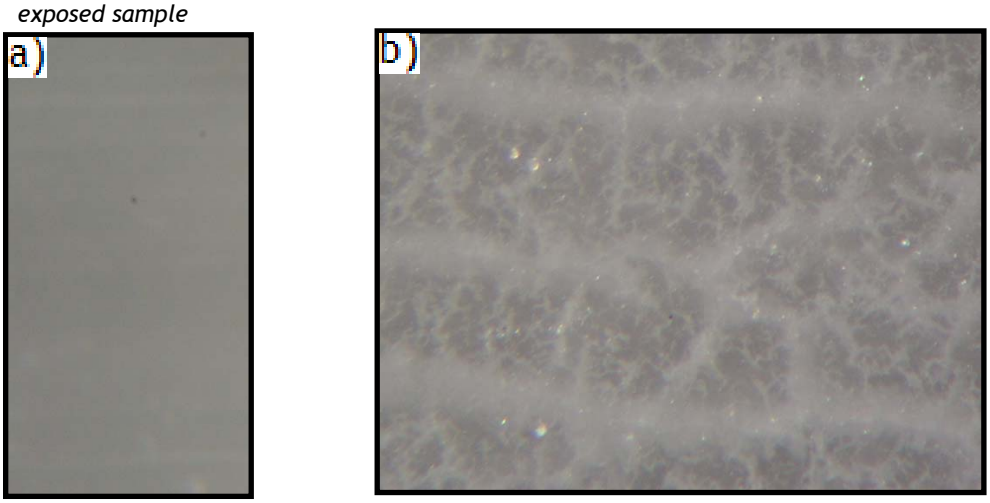

Fig.45: The micrograph of the β-nucleated iPP of MFI=1, a) unexposed, b) 240 hours exposed sample

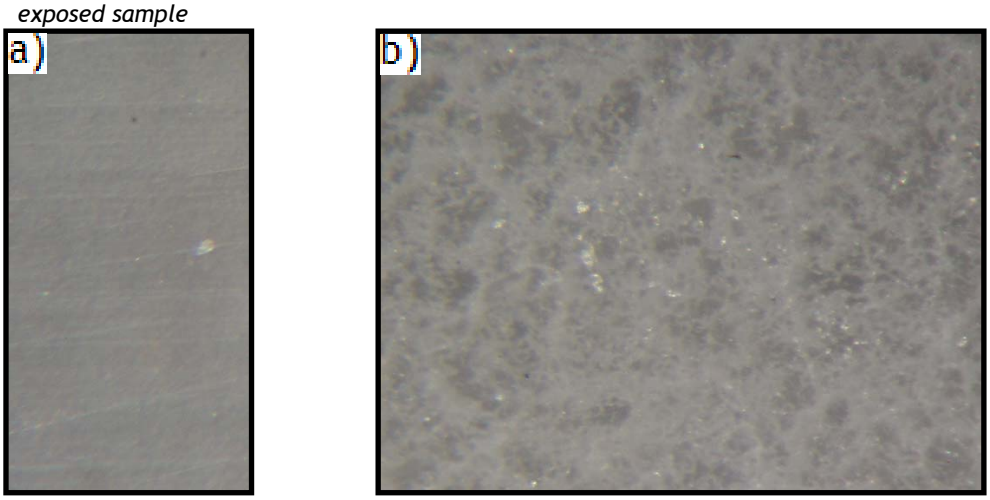

Fig.46: The micrograph of the β-nucleated iPP of MFI=20, a) unexposed, b) 240 hours exposed sample

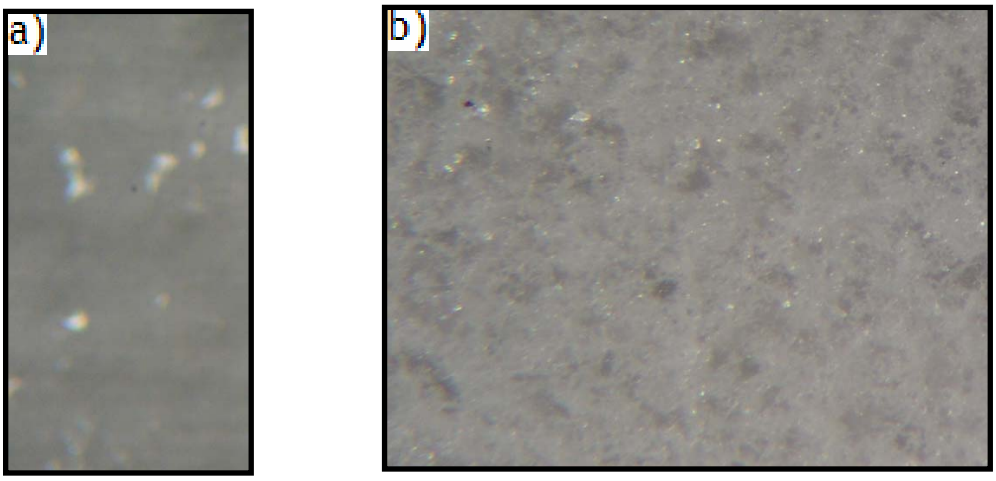

Fig.47: The micrograph of the β-nucleated iPP of MFI=125, a) unexposed, b) 240 hours exposed sample

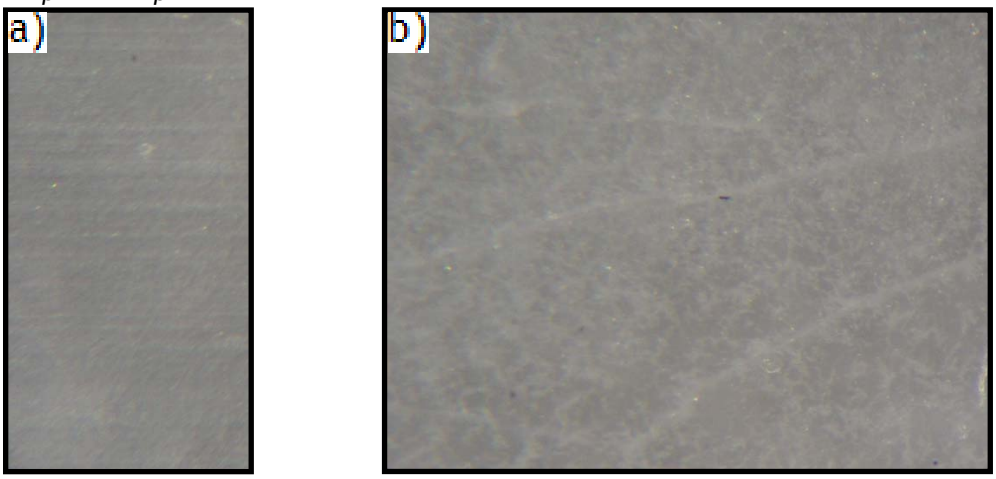

Fig.48: The micrograph of the β-nucleated iPP of MFI=1 200, a) unexposed, b) 240 hours exposed sample

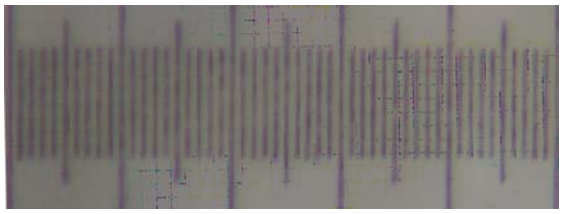

0.5mm

10. DIFFERNETIAL SCANNING CALORIMETRY

Differential scanning calorimetry was used to observe the evolution of melting, re-crystallization and re-melting profiles upon UV-irradiation. The values of melting temperatures, re-crystallization temperatures, re-melting temperatures and heats of phase transitions are plotted in Table B.

10.1 MELTING

The following Figs. 49-53 display melting thermograms of both neat and β-ncleated polypropylenes. The thermograms of neat polypropylenes show only one melting peak which indicates the presence of α-form. On the other hand, two melting peak of β-nucleated polypropylenes indicate, beyond α-form, also the presence of β-form (melting peak with lower melting temperature). It is important to note that the α-melting peak does note that the α-melting peak does not reflect the presence of α-form in original samples but a temporary recrystallization during heating in DSC cell. Indeed, β-form is not stable and recrystallizes into α-phase upon heatig if it is cooled below 100 °C before. This β to α recrystallization seems to be suppressed by UV-irradiation; as exposure time increases the extent of α-melting peak decreases. It can be caused by the introduction of irregularities into polymer chanis during UV-irradiation.

What is also observed in the graphs is gradual decrease of melting temperature with increasing exposure time. The UV-light causes the errosion of the surfaces of the crystallites decreasing their thermodynamic stability and thus their melting temperature. The melting temperature decrease is more pronounced for neat polypropylenes indicating their lower stability against UV-irradiation as compared to β-nucleated polypropylenes (see Table A).

The significant influence of MFI on the melting behaviour is not observed.

The following figures displays melting thermograms for each MFI value both, α-form and β-form polypropylene.

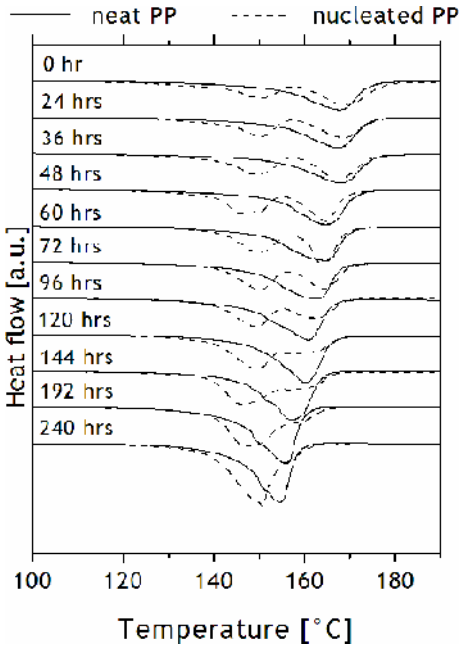

Fig.49: Melting curve of MFI=0.3

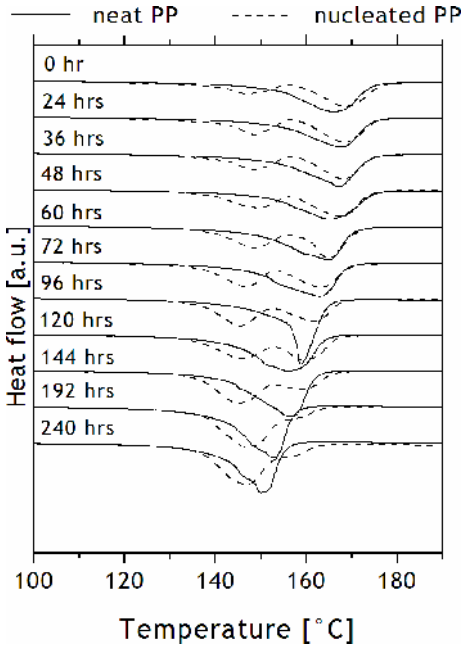

Fig.50: Melting curve of MFI=1

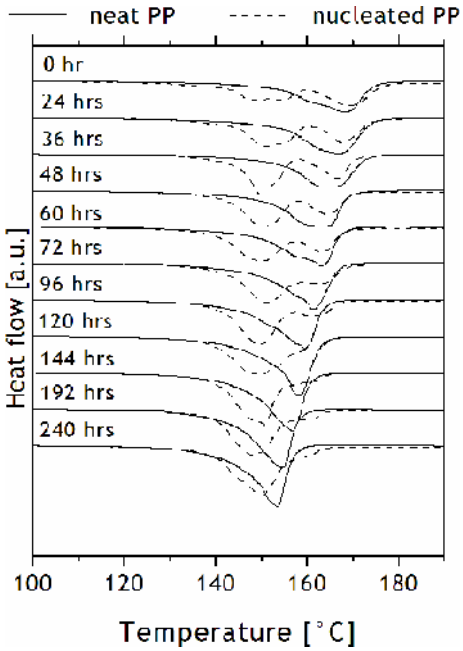

Fig.51: Melting of curve MFI=20

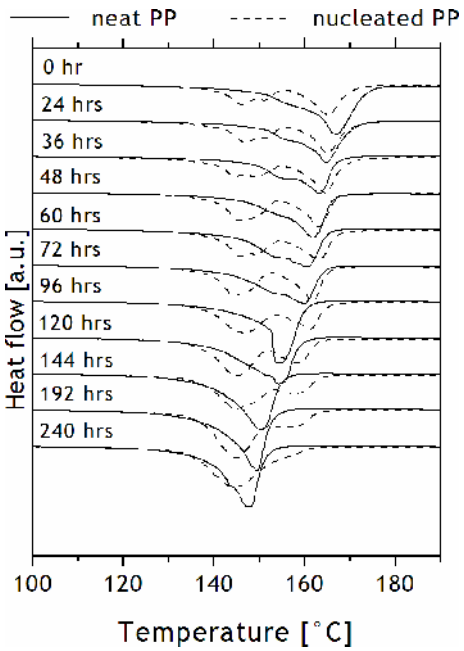

Fig.52: Melting curve of MFI=125

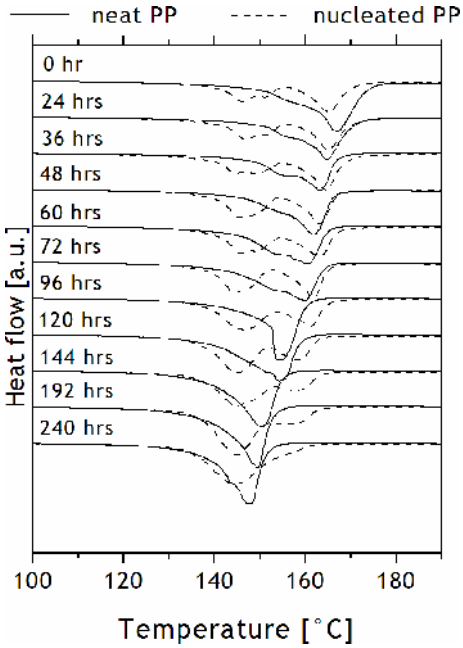

F*ig.53: Melting curve of MFI=1200*

10.2 RE-CRYSTALLIZATION

The melted polypropylenes were then non-isothermally crystallized and the crystallization exotherms of each material are shown in Figs. 54-58. Generally, β-nucleated polypropylenes crystallize at higher crystallization temperature. Indeed, tha addition of heterogeneous nuclei into the material accelerates the crystallization.

Among all materials, the higher crystallization temperatures are observed for polypropylenes with MFI of 120 g/10 min. Thus, the molecules of such material seem to crystallize the most willingly as compared with the others materials.

The evolution of crystallization temperatures upon UV-irradiation is shown in Fig. 59 and 60. It is seen that the crystallization temperature slightly increases at the beginning of irraditation. and subsequently decreases at prolonged exposure. The explanation of this increase consists in the presumption that[79] the decrease in molecular weight due to chain scission upon irradiation can increase the crystallization rate and[80] the chemical irregularities present in the irradiated samples increase the polarity increasing the rate of nucleation.[16] Nevertheless, the high concentration of defects contrariwise inhibits crystallization. Thus, at prolonged exposure time the T_c decreases.

In some cases, the UV-exposure causes the splitting of crystallization exotherms into two peaks (e.g. Fig. 55, nucleated PP irradiated for 144 hrs). Even prolonged irradiation leads to the merging of these individual peaks again into one exotherm but shifted to lower temperature. This behaviour indicated the formation of two crystalline phases differing in the thermodynamic stability.

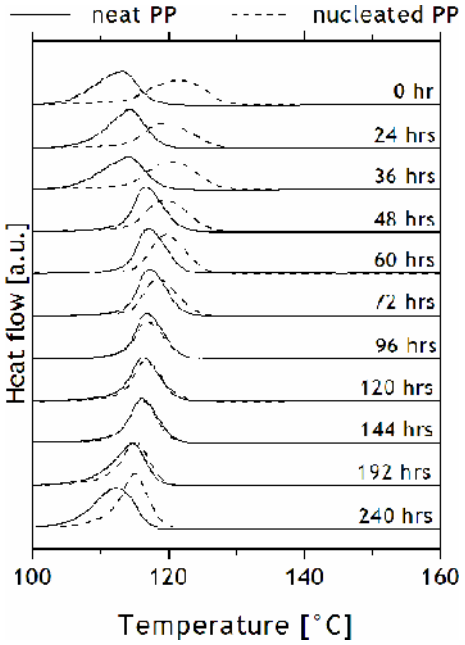

Fig.54: Re-crystallization curve of MFI=0.3

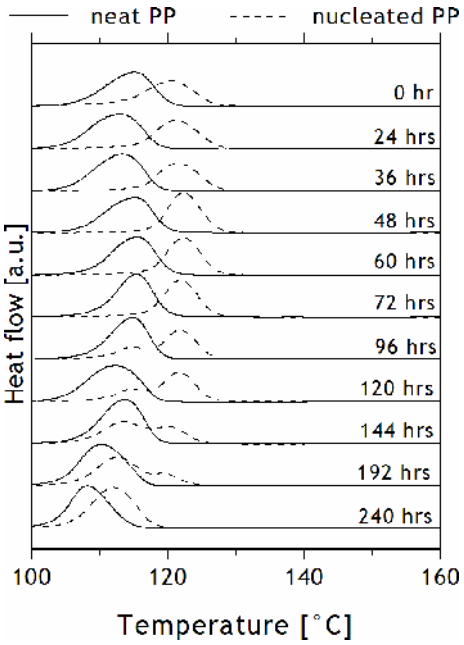

Fig.55: Re-crystallization curve of MFI=1

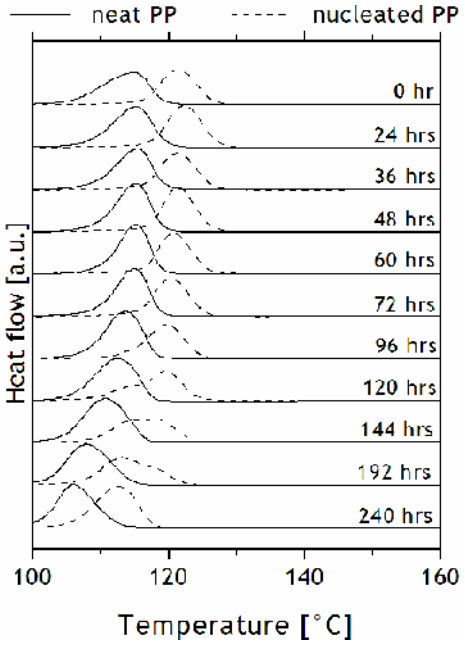

Fig.56: Re-crystallization curve of MFI=20

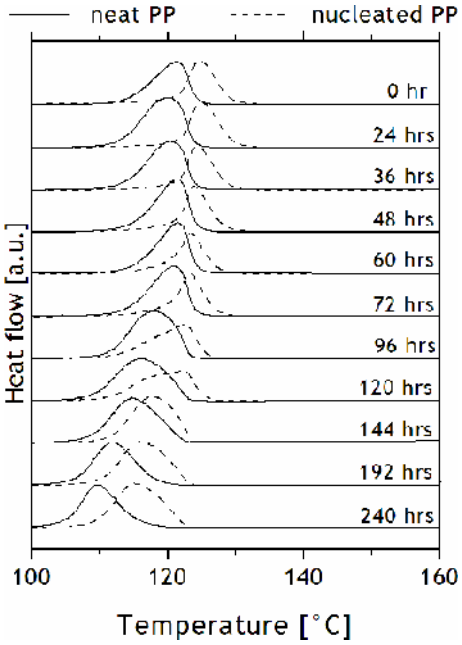

Fig.57: Re-crystallization curve of MFI=125

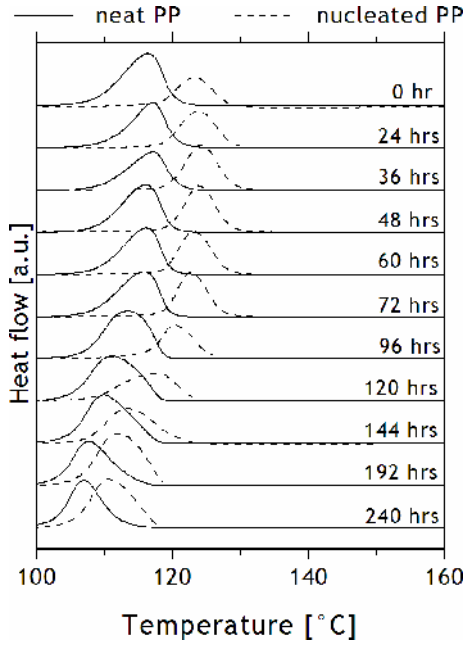

F*ig.58: Re-crystallization curve of MFI=1200*

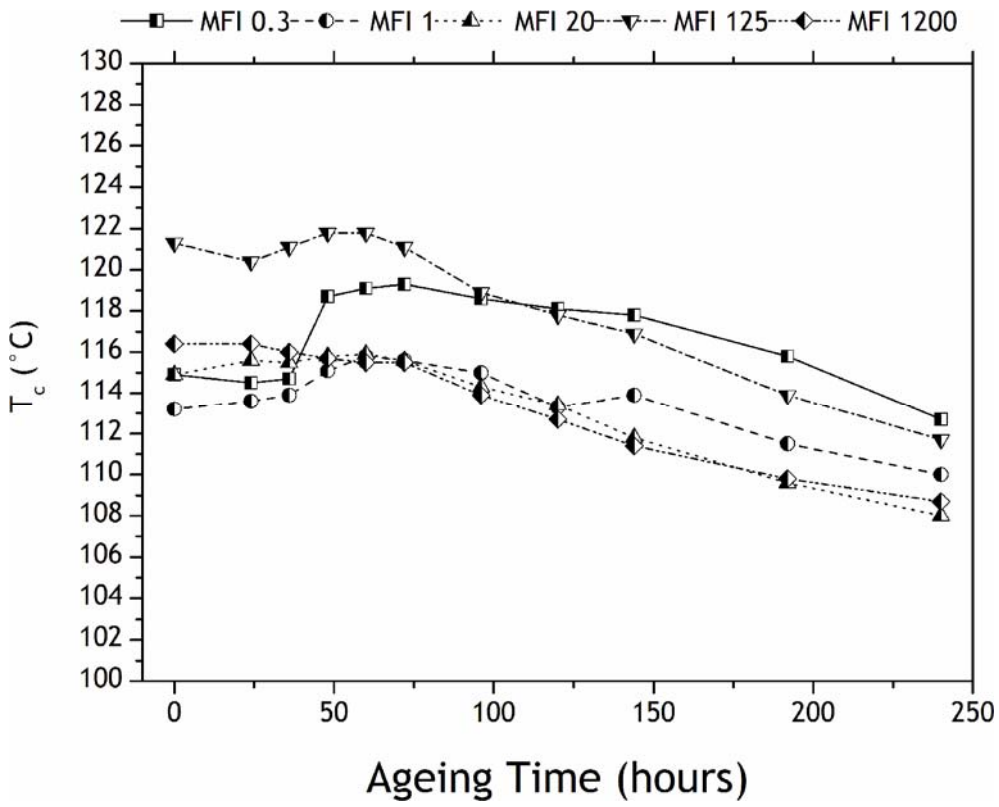

Fig.59: The evolution of crystallization temperature during the irradiation for neat polypropylene

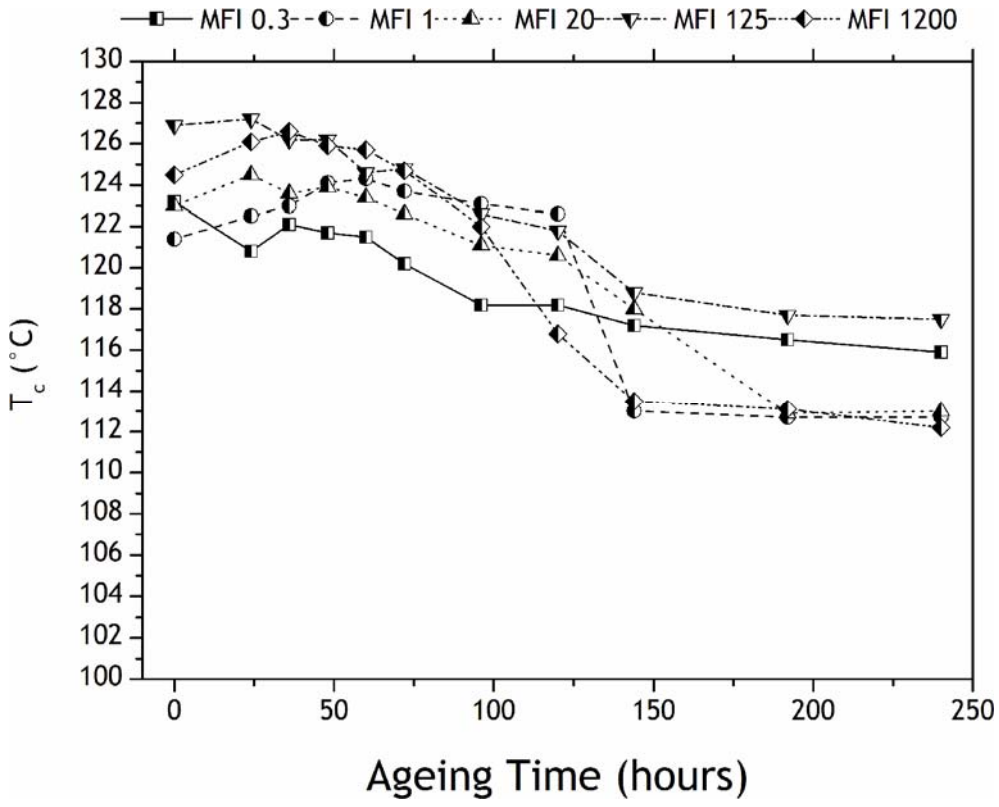

Fig.60: The evolution of crastallization temperature during the irradiation for nucleated polypropylene

10.3 RE-MELTING

Non-isothermally crystallized samples were then re-melted and corresponding thermograms are shown in Figs. 61-65. The profiles of the curves reflect the structure formed during re-crystallization. The general trend observed in all samples is the decrease of melting temperatures caused by the chain scission and an introduction of irregularities into polymer chains. Again, this decrease of melting temperature is more pronounced for neat polypropylenes as compared with β-nucleated ones. In the case of β-nucleated polypropylenes irradiated for a long time (192, 240 hrs) the melting temperature slightly increases. Moreover, the endotherms are very broad or they are splitted. This indicates the presence of two crystalline phases with different thermodynamical stability and it corresponds to the splitted crystallization exotherms.

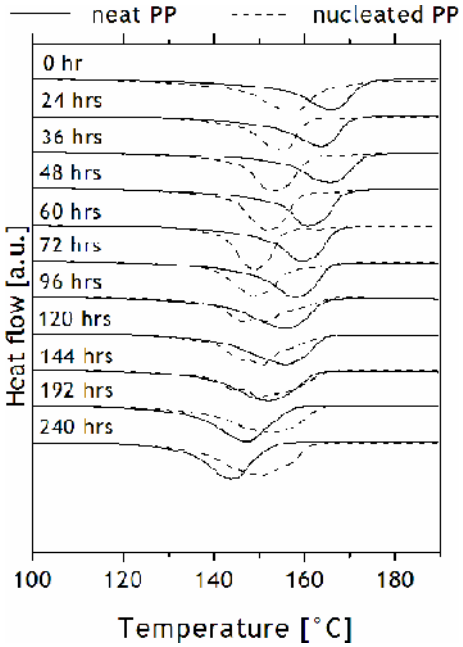

Fig.61: Re-melting curve of MFI=0.3

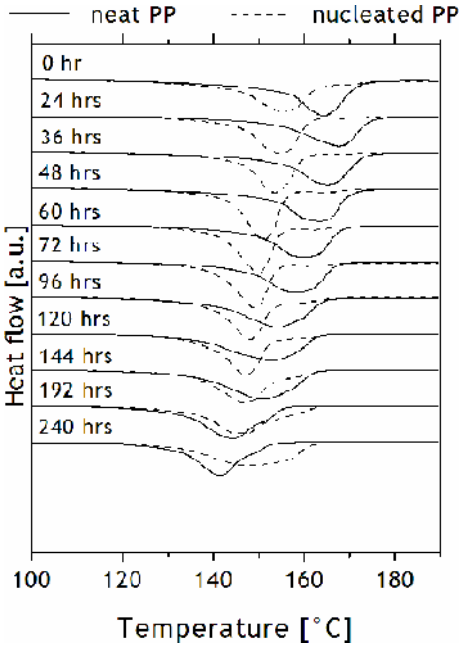

Fig.62: Re-melting curve of MFI=1

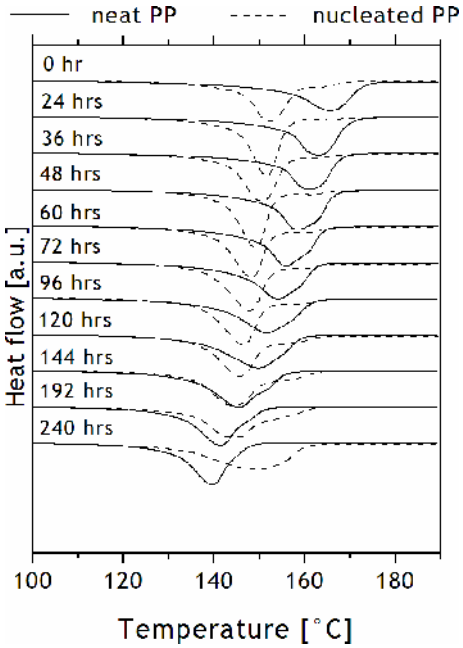

Fig.63: *Re-melting curve of MFI=20*

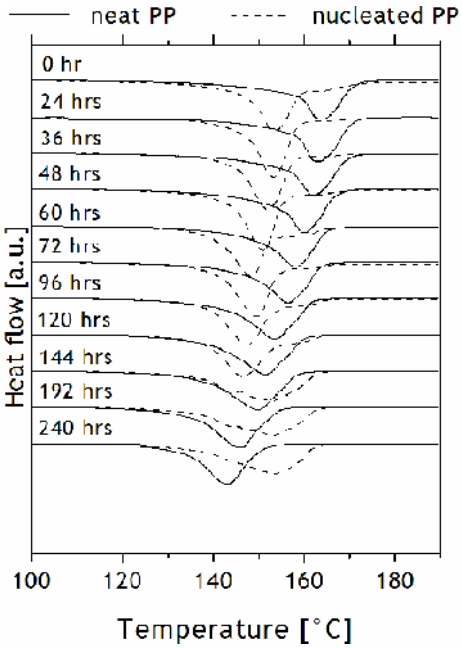

Fig.64: *Re-melting curve of MFI=125*

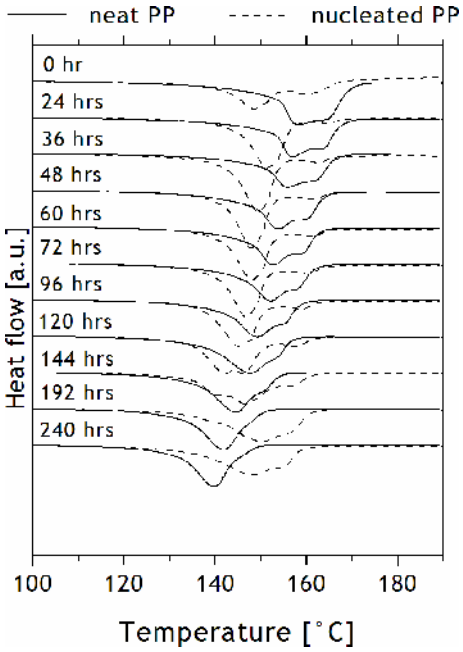

Fig.65: *Re-melting curve of MFI=1200*

CONCLUSIONS

This thesis is focused on the influence of various melt flow indexes of neat and β-nucleated isotactic polypropylenes on UV-degradation. Five wide range values of melt flow indexes were subjected. The samples were exposed to UV-irradiation for several times and the changes were analyzed by infrared spectroscopy, X-ray diffraction, optical microscopy and differential scanning calorimetry.

The results from infrared spectroscopy indicated a distinct resistivity of nucleated and neat polypropylene to the UV-light. β-nucleation led to the improvement of UV-stability of the polypropylene. The definite effect of melt flow indexes on the resistivity and chemical changes (carbonyl index growth) in the material was not unambiguously observed. Only the polypropylene with MFI=0.3 showed significant deviation: its carbonyl index rised markedly at the beginning of irradiation time as compared to the others materials under the study. This trend was observed for both neat and nucleated polypropylenes.

The outcomes from X-ray diffraction measurements indicated the increase of crystallinity with the irradiation time caused by the process of chemi-crystallization. The crystallinity of nucleated samples was slightly higher than that of neat samples.

The stereomicroscope micrographs revealed the introduction of cracks on the surfaces during UV-exposure. The cracks were deeper and more distant for neat polypropylenes as compared to nucleated ones. This corresponded to the larger size of spherulites in neat polypropylenes.

The thermograms of differential scanning calorimetry showed the evolution in changes of melting and crystallization temperatures. The decrease of melting temperature with irradiation time was observed within all samples under the study reflecting the errosion of the surface of the crystallites. This decrease was more pronounced for neat polypropylenes confirming their lower stability than that of β-polypropylene. Re-crystallization temperature reached higher values in the case of nucleated polypropylenes as a consequence of the presence of heterogeneous nuclei in the material. Re-crystallization temperature increased and subseqently decreased during UV-exposure. In some cases, re-crystallization exotherms were doubled. The broadening and splitting of the individual re-melting endotherms reflect the formation of crystallites with lower thermodynamic stability during re-crystallization. This is particularly pronounced for neat polypropylene.

Generally the influence of MFI value of isotactic polypropylene on its UV-degradation was not unambiguously observed. It has to be noted, that the MFI value is not the factor influencing the stability of the material to the UV-degradation. A several factors play role in the process of UV-degradation, neverthless, the most pronounced factor is the presence of β-nucleating agent in the material.

REFERENCES

[1] Turner-Jones A, Aizlewood JM, Beckett DR.; *Makromol. Chem.*; vol. 75; 134; 1964

[2] Brückner, S.; Miele, S. V.; Petraccone, V.; Pirozzi, B.; *Prog. Polym. Sci.*; vol. 16; 361; 1991

[3] Khoury, F. *J.; Res. Nat. Bur. Stand.*; vol. A70; 29; 1966

[4] M. Obadal, R. Čermák, J. Výchopňová, M. Raab, V. Verney, S. Commereuc, F. Fraïsse; *Photodegradability of β-Nucleated Isotactic Polypropylene*. In: 23rd Discussion Conference of P.M.M.; Current And Future Trends in Polymeric Materials*;* Praha; 26.-30. June, 2005

[5] Mark S. M. Alger; *Polymer science dictionary*; New York; 1989

[6] http://www.oehha.ca.gov/air/chronic_rels/pdf/115071.pdf; 1984; 1.5. 2007

[7] http://www.i2t3.unifi.it/spheripol.pdf; 29.10. 2002; 12.2.2005

[8] Burgt, Frank P.T.J. van der; *Crystallization of iPP, The influence of stereo-defects* by Frank P.T.J. van der Burgt.–Eindhoven; Technische Universiteit Eindhoven; ISBN 90-386-2674-6; 2002

[9] Dr. George Benedict; *Metallocene Technology in Commercial Applications*; Society of Plastics; Western reserve University in Cleveland, Ohio; 1980

[10] D. Paukszta, J. Garbarczyk; *Crystallisation of isotactic polypropylene with β-nucleating agents under elevated pressure*; Poznan University of Technology; 5.5.2003; (http://www.fibtex.lodz.pl/44_12_50.pdf; 1.5.2007)

[11] T. Kawai and G. Strobl; *Crystallization Mechanism of sPP;* Physikalisches Institut Albert-Ludwigs-Universität Freiburg, Germany; (http://frsl06.physik.unifreiburg.de/docs/ks.pdf; 10.1.2005)

[12] Obadal M, Čermák R, Baran N, Stoklasa K, Šimoník J.; *Int. Polym. Process*; vol. 19; 35; 2004

[13] Baumhardt-Neto R, DePaoli M. A.; *Polym. Degrad. Stabil.*; vol. 40; 59-64; 1993

[14] http://www.wrap.org.uk/publications/VulnerabilityPolypropylene Photodegradation.pdf (10.1.2005)

[15] Obadal M; Čermák R; Raab M; Verney V; Commereuc S; Fraïsse F; *Study on degradation of β nucleated polypropylenes.* In: IUPAC Macro Meeting; Paris; France; 2004

[16] Obadal M; Čermák R; Raab M; Verney V; Commereuc S; Fraisse F.; *Polym. Deg. Stabil*; vol. 88; 532; 2005

[17] Al-Malaika, S. and Scott, G.; *Photostabilisation of polyolefins*, *Degradation and Stabilisation* of *Polyolefins;* (ed. N.S. Allen); Applied Science; London; pp. 283-336; 1983

[18] Billingham, N.; *Physical phenomena in the oxidation and stabilisation of polymers*, in Oxidation Inhibition of Organic Materials; vol. 11; (eds. P. Klemchuk and J. Pospisil); CRC Press; Boca Raton; FL; pp. 249-298; 1990

[19] Vladislav Hagen; *Únava a stárnutí materiálu*; Brno; 1977

[20] Huihui Li, Xiuqin Zhang, Yongxin Duan, Dujin Wang, Lin Li and Shouke Yan; *Polymer*; Vol. 45; issue 23, 8059-8065; 2004.

[21] Frank P.T.J. van der Burget; *Crystallization of Isotactic Polypropylene : The influence of stereo-defects*; Eindhoven : Technische Universiteit Eindhoven; 2002.

[22] Natta, G. and Corradini, P.; *Structure and properties of isotactic polypropylene*; Nuovo Cimento Suppl; vol. 15; 40-51; 1960

[23] Natta, G.; Corradii, P.; *Suppl. nuovo Cimento*; 15, 40; 1960

[24] E. Lezak, Z. Bartzak; *Fibres and Textiles in Eastern Europe*; vol.13; No 5 (53); 2005

[25] Paul J. Phillips and Khaled Mezghani; *Polypropylene, Isotactic (Polymorphism)*; Department of Materials Science and Engeneering University of Tenessee; 1996

[26] Keith, H. D.; Padden, F.. Jr.; Walter, n. m.; Wyckoff, H. W.; *J. Appl. Phys.*; vol. A2; 398; 1959

[27] Meille S.V., Ferro D.R., Brückner S., Lovinger A.J., Pardem F.J; *Macromolecules*; vol. 27; 2615; 1994

[28] L.A. Utracki; *Polymer Blends Handbook; vol.1: Fundamentals*; Kluwer Academic Publisher; ISBN 1-4020-1110-5

[29] Sehyun Kim and Edwin B. Townsend IV; *β-crystalline polypropylene (BEPOL™) and oriented film aplications*; Polypropylene Product Development Sunoco Chemicals Research and Technology Department 550 Technology Drive, Pittsburgh; PA 15219 (http://www.4spe.org/membercenter/library/samples/2002-00059.pdf; 1.5.2007))

[30] Kotek J, Raab M, Baldrian J, Grellmann W; J. Appl. Polym. Sci.; vol 85; 1174–1184; 2002

[31] Obadal M, Čermák R, Baran N, Stoklasa K, Šimoník J. Int. Polym. Process; vol. 19; 35–39; 2004

[32] Výchopňová J, Habrová V, Obadal M, Čermák R, Čabla R; J *Therm. Anal. Calorim*; vol. 86; 687–691; 2006

[33] Marco C, Gomez MA, Ellis G, Arribas JM; *J. Appl. Polym. Sci.*; vol. 86; 531–539; 2002

[34] Varga J, Menyhárd A.; *Macromolecules 2007*; in press

[35] Varga, J.; *Crystallization*; *Melting and Supermolecular Structure of Isotactic Polypropylene. In Polypropylene: Structure, Blends and Composites*; Karger-Kocsis, J., Ed.; vol. 1, 56–115; Chapman & Hall: London; 1995

[36] Shi, G.; Zhang, X.; Qiu, Z; *Makromol. Chem.; vol.* 193; 583–591; 1992

[37] Varga, J; *Supermolecular Structure of Isotactic Polypropylene;* vol. 27; 2557–2579; J. Mater. Sci.; 1992

[38] Varga, J.; Schulek-Toth, F.; Ille, A; *Effect of Fusion Condition of β-Polypropylene on New Crystallization;* vol. 269, 655–664; 1991

[39] Padden, F.J.; Keith, H.D.; Colloid Polym. Sci.; vol. 30; 1479–1484.(2); 1959

[40] Norton, D.R.; Keller, A.; *Polymer;* vol. 26; 704–716; 1985

[41] Shi, G.; Huang, B.; Zhang, *J; Makromol. Chem. Rapid Commun*; *Enthalpy of Fusion and Equilibrium Melting Point of the β-Form of Polypropylene;* vol. 5; 573–578; 1984

[42] Zhou, G.; He, Z.; Yu, J.; Han, Z.; Shi, G.; *Makromol. Chem.;* vol. 187; 633–642; 1986

[43] Shi, G.; Huang, B.; Cao, Y.; He, Z.; Han, Z. ; *Makromol. Chem.*; vol. 117; 643–652; 1986

[44] Varga, J; *J. Therm. Anal.;* vol. 31; 165–172; 1986

[45] Bruckner, S. and Meille, S.V; *Nature;* vol. 340; 455-457; 1989

[46] Bruckner, S. and Meille, S.V, Petraccone, V., and Pirozzi, B.; *Prog. Polym. Sci.*; vol. 16; 361-404; 1991

[47] Maier, C. - Calafut, T.: *Polypropylene - The Definitive User's Guide and Databook*; Plastics Design Library; ISBN: 1884207588; 1998

[48] Varga, J.; *Jour. of Macromolecular Science - Physics*, vol. B41, 1121 – 1171; 2002

[49] K. P. Blackmon, L. P. Barthel-Rosa, S. A.Malbari, D. J. Rauscher, andM.M. Daumerie; *Production of ultra high melt flow polypropylene resins*, US Patent 6 657 025; assigned to Fina Technology; Inc. (Houston, TX); December 2; 2003.

[50] Ing. Zdeněk Zámorský, CSc; *Nauka o polymerech*; Brno; 1980

[51] Zeus, *Weathering of Plastics,* (technical whitepaper: http://www.zeusinc.com/pdf/Zeus_Weathering_of_Plastics.pdf; 1.5.2005)

[52] Varga, J.; Schulek-Toth, F.; Ille, A.; ; *Colloid Polym. Sci.;* vol. 269; 655–664; 1991

[53] Břetislav Doležel; *Odolnost plastů a pryží*; Praha; 1981

[54] J. Karger-Kocsis; *Polypropylene-An A-Z Reference*; Kluwer Academic Publishers; 566-568; ISBN10: 0412802007; 1999

[55] Béla Pukánzsky; *Polypropylene-An A-Z Reference*; Edited by J. Karge-Kocsis; Kluwer Academic Publishers; 574-577; ; ISBN10: 0412802007; 1999

[56] Rabello, M. S., White, J. R.; *Polym. Degrad. Stab.*; vol. 56; 55; 1997

[57] Rabello, M. S., White, J. R.; *Polymer;* vol. 38; 6389; 1997

[58] McTigue, F. H., Blumberg, M.; *j Appl. Polym. Sci., Appl. Polym. Symp.*; vol. 4; 175; 1967

[59] Ogier, L. Rabello, M. S., White, J. R.; *J Mater. Sci.*; vol. 30; 2364; 1995

[60] M. S. Rabello, J. R. White; *Polym. Degrad. Stabil.*; vol. 56; Number 1, April 1997, pp. 55-73(19); Elsevier; 1996

[61] Martin Obadal, Roman Čermák, Miroslav Raabb, Vincent Verneyc,Sophie Commereucc, Frederic Fraisse; *Pol. Degrad. Stabil.*; vol. 88; 532-539; 2005

[62] Baumhardt-Neto R, DePaoli M. A.; *Polym. Degrad. Stabil.*; vol. 40; 59-64; 1993

[63] J. Karger-Kocsis; *Polypropylene-An A-Z Reference*; Kluwer Academic Publishers; 1998

[64] Rabello MS, White JR.; *Polym. Degrad. Stabil.*; vol. 56; 55-73; 1997

[65] en.wikipedia.org/wiki/Infrared_spectroscopy (1.5.2007)

[66] http://mvh.sr.unh.edu/mvhtools/images/irdiagram.pn; (10.11.2006)

[67] C.-P. Herman Hsu, Ph.D., *Infrared spectroscopy,* Separation Sciences, Research and produkt development Mallinckrodt, Inc. Mallinckrodt Baker Division. (www.prenhall.com/settle/chapters/ch15.pdf; 1.5.2007)

[68] Brian M. Tissue; *X-ray Diffraction*; 2000; (http://elchem.kaist.ac.kr/vt/chem-ed/diffract/xray.htm; 1.5.2007)

[69] Guest Article by Sampath S. Iyengar; *Analysis of Materials by X-Ray Diffraction*; Technology of Materials - 909.471.8194

[70] http://www.mrsec.wisc.edu/Edetc/modules/xray/X-raystm.pdf (1.5.2007)

[71] Dean, John A; *The Analytical Chemistry Handbook*; New York. McGraw Hill; pp. 15.1–15.5; 1995

[72] Pungor, Erno; *A Practical Guide to Instrumental Analysis*; Boca Raton, Florida. 1995. pp. 181–191.

[73] Skoog, Douglas A., F; James Holler and Timothy Nieman. *Principles of Instrumental Analysis*. Fith Edition. New York; pp. 905–908; 1998

[74] www.colby.edu/chemistry/PChem/lab/DiffScanningCal.pdf; (1.5.2007)

[75] http://en.wikipedia.org/wiki/Optical_microscope; (1.5.2007)

[76] http://people.ccmr.cornell.edu/~mseugrad/micro/images/microoptics.gif (1.5.2007)

[77] Lenka Chvatalova; *On Efficiency of Specific Nucleation in Polypropylene;* Master Thesis*;* 2006

[78] Delprat P, Duteurtre X, Gardette JL. *Polym. Degrad. Stabil.*; vol. 50: 1-12. ; 1995

[79] Singh RP, Mani R, Sivaram S, Lacoste J, Vaillant D; *J. Appl. Polym. Sci*; vol. 50; 1871-81; 1993

[80] M. S. Rabello and J. R. White; *Polymer*; vol. 38; Issue 26; 6389-6399; 1997

REVIEW OF SYMBOLS

pp	Polypropylene
aPP	Atactic polypropylene
sPP	Syndiotactic polypropylene
iPP	Isotactic polypropylene
α	Monoclinic crystalline phase
α_I	Positive birefringent spherulites
α_{II}	Negative birefringent spherulites
α_{III}	Mixed birefringent spherulites
α_m	Mixed birefringent spherulites
β	Trigonal crystalline form
γ	Orthorhombic crystalline form
α-iPP	Polypropylene containing mainly α-form
β-iPP	Polypropylene containing mainly β-form
T_c	Crystllization temperature [°C]
T_m°	Equilibrium melting temperature [°C]
T_g	Glass transition temperature [°C]
T_m	Melting temperature [°C]
T_R *	Critical recooling temperature [°C]
T($\beta\alpha$)	High-temperature $\beta\alpha$-growth transition
T($\alpha\beta$)	Low-temperature $\beta\alpha$-growth transition
ABS	Acrylonitrile butadiene styrene
SMS	Supermolecular structure
ρ	Density [kg/m^3]
SAXS	Small-angle X-ray scattering
WAXS	Wide-angle X-ray scattering
G_α	Growth rate of α-phase [s^{-1}]
G_β	Growth rate of β-phase
MFI	Melt flow index [g/min]
M_r	Relative molecular weight
Mw/Mn	Molecular weight distribution
UV	Ultraviolet
MFI	Melt flow index
IR	Infrared
E	Energy of radiation [J]

f	Frequency of radiation [1/s]
h	Planck's constant [J.s]
λ	Wavelength [nm]
FTIR	Fourier transform infrared spectroscopy
DSC	Differential scanning calorimetry
d	Spacing between the planes in the atomic lattice [nm]
n	Integer
Θ	Angle of X-ray diffraction
d	Resolution
A_N	Numerical aperture
3-D	Three dimensional
X_C	Crystallinity
K_α	Content of α-form
K_β	Content of ß-form
K_γ	Content of γ-form
T_{m1}	The first meting temperature [°C]
T_{m2}	The re-melting temperature [°C]
ΔH_{m1}	**M**elting enthalpy [J]
ΔH_c	Crystallization enthalpy [J]
ΔH_{m2}	Re-melting enthalpy [J]
$H_{\alpha 1}$	Intensity of α-diffraction peak
$H_{\alpha 2}$	Intensity of α-diffraction peak
$H_{\alpha 2}$	Intensity of α-diffraction peak
H_β	Intensity of ß-diffraction peak
I	Total ratio of integral intensities diffracted by a crystalline part
I_c	Intensity diffracted by a crystalline part

REVIEW OF FIGURES

REVIEW OF TABLES

LIST OF APPENDICES

Table A: The evaluated data of X-ray measurement

Irradiation time	MFI=0.3; 0 NU 100				MFI=1; 0 NU 100				MFI 20; 0 NU 100				MFI 125; 0 NU 100				MFI=1200; 0 NU 100			
	X_c	K_α	K_β	K_γ	X_c	K_α	K_β	K_γ	X_c	K_α	K_β	K_γ	X_c	K_α	K_β	K_γ	X_c	K_α	K_β	K_γ
0	0.49	0.97	0.03	0	0.47	1	0	0	0.50	1	0	0	0.51	1	0	0	0.54	1	0	0
24	0.49	0.96	0.04	0	0.47	1	0	0	0.50	1	0	0	0.53	1	0	0	0.55	1	0	0
36	0.51	0.97	0.03	0	0.51	1	0	0	0.53	1	0	0	0.53	1	0	0	0.55	1	0	0
48	0.53	0.96	0.04	0	0.52	1	0	0	0.52	1	0	0	0.51	1	0	0	0.56	1	0	0
60	0.54	0.97	0.03	0	0.52	1	0	0	0.54	1	0	0	0.52	1	0	0	0.55	1	0	0
72	0.56	0.96	0.04	0	0.54	1	0	0	0.54	1	0	0	0.54	1	0	0	0.56	1	0	0
96	0.54	0.96	0.04	0	0.55	1	0	0	0.55	1	0	0	0.54	1	0	0	0.59	1	0	0
120	0.57	0.96	0.04	0	0.56	1	0	0	0.56	1	0	0	0.55	1	0	0	0.56	1	0	0
144	0.56	0.96	0.04	0	0.54	1	0	0	0.56	1	0	0	0.54	1	0	0	0.57	1	0	0
192	0.55	0.96	0.04	0	0.54	1	0	0	0.56	1	0	0	0.53	1	0	0	0.55	1	0	0
240	0.55	0.96	0.04	0	0.54	1	0	0	0.55	1	0	0	0.55	1	0	0	0.56	1	0	0
Irradiation time	MFI=0.3; 0.03 NU 100				MFI=1; 0.03 NU 100				MFI=20; 0.03 NU 100				MFI=125; 0.03 NU 100				MFI=1200; 0.03 NU 100			
	X_c	K_α	K_β	K_γ	X_c	K_α	K_β	K_γ	X_c	K_α	K_β	K_γ	X_c	K_α	K_β	K_γ	X_c	K_α	K_β	K_γ
0	0.55	0.10	0.90	0	0.45	0.11	0.89	0	0.51	0.06	0.94	0	0.56	0.06	0.94	0	0.53	0.07	0.93	0
24	0.58	0.09	0.91	0	0.49	0.11	0.89	0	0.51	0.02	0.98	0	0.59	0.07	0.93	0	0.55	0.07	0.93	0
36	0.57	0.09	0.91	0	0.5	0.11	0.89	0	0.54	0.05	0.95	0	0.62	0.06	0.94	0	0.60	0.08	0.92	0
48	0.58	0.09	0.91	0	0.51	0.11	0.89	0	0.58	0.06	0.94	0	0.62	0.06	0.94	0	0.56	0.07	0.93	0
60	0.59	0.09	0.91	0	0.5	0.11	0.89	0	0.55	0.06	0.94	0	0.60	0.06	0.94	0	0.56	0.07	0.93	0
72	0.60	0.09	0.91	0	0.52	0.11	0.89	0	0.56	0.02	0.98	0	0.62	0.07	0.93	0	0.55	0.06	0.94	0
96	0.59	0.09	0.91	0	0.52	0.11	0.89	0	0.60	0.03	0.97	0	0.59	0.06	0.94	0	0.57	0.07	0.93	0
120	0.59	0.09	0.91	0	0.52	0.11	0.89	0	0.61	0.06	0.94	0	0.63	0.07	0.93	0	0.57	0.07	0.93	0
144	0.61	0.09	0.91	0	0.54	0.1	0.90	0	0.55	0.05	0.95	0	0.60	0.06	0.94	0	0.57	0.07	0.93	0
192	0.63	0.09	0.91	0	0.51	0.1	0.90	0	0.57	0.06	0.94	0	0.61	0.06	0.94	0	0.57	0.07	0.93	0
240	0.62	0.09	0.91	0	0.53	0.11	0.89	0	0.56	0.06	0.94	0	0.60	0.06	0.94	0	0.57	0.07	0.93	0

Table B: Crystallization and melting characteristics of samples surveyed by DSC method

Irradiation time [h]	Sample	T_{m1} [°C]		ΔH_{m1} [mJ]	T_c [°C]	ΔH_c [mJ]	T_{m2} [°C]		ΔH_{m2} [mJ]
		α-form	β-form				α-form	β-form	
0	0 NU 100								
	ITT 0.3	167.7		879	114.9	888	165.6		880.3
	ITT 1	167.6		890	113.2	865	165.9		876.9
	ITT 20	166.1		942	114.9	970	163.8		975.1
	ITT 120	168.4		863	121.3	881	163.7		893
	ITT 1200	167.1		1187	116.4	1192	158.4		1222.2
	0.03 NU 100								
	ITT 0.3	168.6	144.1	1176	123.2	1103		156.3	1168.1
	ITT 1	168.8	145	820	121.4	782		154.3	857.1
	ITT 20	168.1	148.5	809	123	782		151.3	851.9
	ITT 120	169.3	148.8	931	126.9	935		152.2	1013.7
	ITT 1200	165.7	145.6	891	124.5	729		148	848.9

Irradiation time [h]	Sample	T_{m1} [°C]		ΔH_{m1} [mJ]	T_c [°C]	ΔH_c [mJ]	T_{m2} [°C]		ΔH_{m2} [mJ]
		α-form	β-form				α-form	β-form	
24	0 NU 100								
	ITT 0.3	167.6		778.2	114.5	809.5	163		806.9
	ITT 1	167.6		1023.1	113.6	1052.5	164.9		1050.9
	ITT 20	166.4		899.2	115.6	966.7	162.8		969.5
	ITT 120	166.7		873.9	120.4	885.7	162.8		901.3
	ITT 1200	164.8		873.6	116.4	855.66	157.1		901.9
	0.03 NU 100								
	ITT 0.3	168.6	149.6	991.8	120.8	922		154.3	1026.9
	ITT 1	168.6	148.1	1046.8	122.5	871.2		153.6	917.5
	ITT 20	167.12	149.5	938.7	124.5	856.9		150.1	968.9
	ITT 120	167.7	150.1	1053.3	127.2	873.7		151.7	1007.5
	ITT 1200	165.3	146.3	1154.4	126.1	1074.5		149.8	1172.3

Irradiation time [h]	Sample	T_{m1} [°C]		DH_{m1} [mJ]	T_c [°C]	DH_c [mJ]	T_{m2} [°C]		DH_{m2} [mJ]
		a-form	b-form				a-form	b-form	
36	0 NU 100								
	ITT 0.3	167.8		985	114.7	1012.8	165.6		1022.9
	ITT 1	166.8		972.9	113.9	1016.9	164.5		1013
	ITT 20	165.5		788.7	115.5	826.7	160.8		826.6
	ITT 120	164.9		985	121.1	985.6	161.6		1022.9
	ITT 1200	163.2		775	116	764.8	156.3		796
	0.03 NU 100								
	ITT 0.3	167.2	148.9	1069.2	122.1	980		151.6	1094.5
	ITT 1	168.3	147.8	924.8	123	887.8		152	975.2
	ITT 20	165.6	148.7	1119.7	123.6	988.3		149	1109.3
	ITT 120	166.8	149	941.6	126.2	862.2		150.4	946.3
	ITT 1200	164.7	144.4	1103.5	126.6	988		147.9	1074.3

Table B: continued

Irradiation time [h]	Sample	T_{m1} [°C]		ΔH_{m1} [mJ]	T_c [°C]	ΔH_c [mJ]	T_{m2} [°C]		ΔH_{m2} [mJ]
		α-form	β-form				α-form	β-form	
48	0 NU 100								
	ITT 0.3	164.4		1020.1	118.7	979	160.2		1031.7
	ITT 1	165.1		895.5	115.1	938.9	162.8		957.5
	ITT 20	164.4		919.6	115.8	918.8	158		933.9
	ITT 120	163.4		1040.5	121.8	969.1	159.3		1001.4
	ITT 1200	161,4		981,9	115,7	945,5	153,3		960,2
	0.03 NU 100								
	ITT 0.3	166.6	149.6	1343.6	121.7	1194.6		149.6	1315.5
	ITT 1	167.5	149.2	876.5	124.1	800.1		149.6	888.1
	ITT 20	161.9	149.4	1198.6	123.9	960.7		147.5	1073.9
	ITT 120	164.6	149.7	1263.4	126.2	1092.3		148.8	1201.5
	ITT 1200	162.8	144.8	872	125.9	775.4		146.7	865.7

Irradiation time [h]	Sample	T_{m1} [°C]		ΔH_{m1} [mJ]	T_c [°C]	ΔH_c [mJ]	T_{m2} [°C]		ΔH_{m2} [mJ]
		α-form	β-form				α-form	β-form	
60	0 NU 100								
	ITT 0.3	164.4		1009.7	119.1	945.5	158.7		987.5
	ITT 1	165		996.6	115.8	976.5	159.2		984.4
	ITT 20	161.5		936.1	115.9	910.8	155.1		931.9
	ITT 120	162.6		957.7	121.8	918.6	157.2		937.9
	ITT 1200	160		943.2	115.5	871.1	152.2		895.4
	0.03 NU 100								
	ITT 0.3	163.3	149.1	1053.1	121.5	857.7		147.7	945.6
	ITT 1	165	148.2	1033.4	124.3	865.8		148.3	967.7
	ITT 20	159.6	149.1	1339.5	123.4	1092.8		146.3	1202.8
	ITT 120	163.4	149.3	1138.6	124.6	962.3		146.8	1036.9
	ITT 1200	163.3	144.9	1163	125.7	1017.8		146.4	111.7

Irradiation time [h]	Sample	T_{m1} [°C]		ΔH_{m1} [mJ]	T_c [°C]	ΔH_c [mJ]	T_{m2} [°C]		ΔH_{m2} [mJ]
		α-form	β-form				α-form	β-form	
72	0 NU 100								
	ITT 0.3	162.6		1033	119.3	935.4	157.1		981.6
	ITT 1	163		1002.6	115.6	929.3	157.3		952.9
	ITT 20	158.9		1039.3	115.6	934.1	153.3		968.9
	ITT 120	160.7		988.7	121.1	883.7	155.7		901.4
	ITT 1200	159.6		1107.8	115.5	999.6	151.3		1012
	0.03 NU 100								
	ITT 0.3	164.3	149.4	904.6	120.2	772.8		147.7	853.2
	ITT 1	163.3	145.8	896.7	123.7	761		147.7	843.2
	ITT 20	162.6	147.4	1303.5	122.6	1077.3		146.2	1181.6
	ITT 120	165.7	149.9	1248.9	124.8	1048.1		147.5	1139.3
	ITT 1200	161.8	144.1	888.2	124.7	771		145.6	838.5

Table B: continued

Irradiation time [h]	Sample	T_{m1} [°C]		ΔH_{m1} [mJ]	T_c [°C]	ΔH_c [mJ]	T_{m2} [°C]		ΔH_{m2} [mJ]
		α-form	β-form				α-form	β-form	
96	0 NU 100								
	ITT 0.3	160.1		1039.9	118.6	930	155.1		938.4
	ITT 1	157.5		1031.9	115	883.3	153.3		906.4
	ITT 20	156.6		1083.1	114.3	926.6	151		971.5
	ITT 120	158.6		1028.6	118.9	883.1	152.7		903.8
	ITT 1200	152.9		973.5	113.9	840.8	148.6		862.6
	0.03 NU 100								
	ITT 0.3	162.7	148.5	919.5	118.2	747.4		145.8	979.5
	ITT 1	162.3	144.8	913	123.1	756.5		146.7	824.8
	ITT 20	161.9	147.1	1055.8	121.1	865		145.2	942.3
	ITT 120	163.1	148.5	1051.6	122.6	871.6		146.1	946.9
	ITT 1200	161	145.9	1216.1	122	993.2		143.7	1100.4

Irradiation time [h]	Sample	T_{m1} [°C]		ΔH_{m1} [mJ]	T_c [°C]	ΔH_c [mJ]	T_{m2} [°C]		ΔH_{m2} [mJ]
		α-form	β-form				α-form	β-form	
120	0 NU 100								
	ITT 0.3	159.3		1141.9	118.1	1039.5	154.8		1073.3
	ITT 1	155		1423.8	113.3	1198.6	151.8		1205.4
	ITT 20	153.5		1244.2	113.4	1021.3	148.9		1030.8
	ITT 120	156.6		1363	117.8	1118.9	150.2		1160.6
	ITT 1200	153.3		1231.9	112.7	1040.9	146.8		1044.6
	0.03 NU 100								
	ITT 0.3	162.7	148.6	1067.8	118.2	900.5		149.5	960.5
	ITT 1	157.8	145.5	752.8	122.6	622		146.1	681.3
	ITT 20	161.6	146	989.9	120.6	789		144.5	870.2
	ITT 120	162.7	148.8	1023.1	121.8	840.7		145.4	906
	ITT 1200	158.2	144.3	970.6	116.8	800.4		145.5	867.7

Irradiation time [h]	Sample	T_{m1} [°C]		ΔH_{m1} [mJ]	T_c [°C]	ΔH_c [mJ]	T_{m2} [°C]		ΔH_{m2} [mJ]
		α-form	β-form				α-form	β-form	
144	0 NU 100								
	ITT 0.3	156		1274.3	117.8	1039.9	151.1		1078.8
	ITT 1	155.4		1121.1	113.9	914.5	150		933.4
	ITT 20	151.3		1227.2	111.8	965.3	144.6		967.5
	ITT 120	155.3		1271	116.9	1025.8	148.6		1051.9
	ITT 1200	149.2		943.3	111.4	762	143.8		774.1
	0.03 NU 100								
	ITT 0.3	161.1	145.7	984.7	117.2	864.1		149.2	887.9
	ITT 1	159.6	144.3	1253.8	113	996.7		145.6	1053.2
	ITT 20	160.3	145.2	967	118	771.5		143.3	830.3
	ITT 120	162	149.4	1026.6	118.8	867.3		152.3	904.3
	ITT 1200	158.5	144	1057.3	113.5	869.3		145.8	921

Table B: continued

Irradiation time [h]	Sample	T_{m1} [°C]		ΔH_{m1} [mJ]	T_c [°C]	ΔH_c [mJ]	T_{m2} [°C]		ΔH_{m2} [mJ]
		α-form	β-form				α-form	β-form	
192	0 NU 100								
	ITT 0.3	154.6		1326.1	115.8	1035.1	146.1		1045.9
	ITT 1	151.5		1226.6	111.5	920.1	143.1		952.6
	ITT 20	148.8		1292.2	109.6	945	140.4		959.6
	ITT 120	153.3		1159.1	113.9	887.1	144.8		913.7
	ITT 1200	147.9		1086.3	109.8	840.8	140.8		840.6
	0.03 NU 100								
	ITT 0.3	146.3	159.3	1203.8	116.5	1021.5		152.6	1025.11
	ITT 1	145.2	160.2	1219.5	112.7	975.6		146.3	1008.3
	ITT 20	145.5	159.8	1049.2	112.9	829.4		142.2	862.4
	ITT 120	161.4	146.7	1065.9	117.7	898.1		152.4	907.4
	ITT 1200	159.8	145.5	1109	113.1	966.3		149.6	997.1

Irradiation time [h]	Sample	T_{m1} [°C]		ΔH_{m1} [mJ]	T_c [°C]	ΔH_c [mJ]	T_{m2} [°C]		ΔH_{m2} [mJ]
		α-form	β-form				α-form	β-form	
240	0 NU 100								
	ITT 0.3	153.1		1237	112.7	937.5	142.7		951.9
	ITT 1	148.9		1029.2	110	788.1	140.4		784.9
	ITT 20	147.5		1167.8	108	855	138.5		866.2
	ITT 120	151.9		1111.7	111.7	828.3	141.9		841.3
	ITT 1200	146.7		836.9	108.7	643.1	139		640.2
	0.03 NU 100								
	ITT 0.3	149.5		1049.7	115.9	842.7	149.7		880.8
	ITT 1	145.7	158.1	1057.3	112.7	867.7	148.5		877.8
	ITT 20	143.9		1032.6	113	848.2	149.4		850.4
	ITT 120	148.7		1325.9	117.5	1116.3	152.6		1138.1
	ITT 1200	143.3		1076.1	112.2	898.6	147.5		922.4